6.0 PROBABILISTIC MODELLING

This chapter outlines the probabilistic hazard model included in this report, and presents the main results. It is intended to provide a general overview of the hazard model, suitable for non-specialists. Additional technical details of the hazard model are presented in Appendix 7.

6.1 INTRODUCTION AND MOTIVATION

There are many ways in which the risks caused by natural hazards can be mitigated; in the case of tsunami these include early-warning systems, evacuation mapping, public education in self-evacuation, land-use zoning, and engineered sea defences. However these techniques must be used appropriately to ensure that mitigation measures are effective in their operation and are suitably prioritised relative to mitigation of other natural and man-made hazards.

A probabilistic assessment of risk, defined as an estimate of the probable economic losses or human casualties in a period of time, is generally considered the best way to make comparisons across multiple hazards.

The relationship between risk, hazard, exposure and vulnerability is, in general terms, defined as:

Risk = Hazard x Exposure x Vulnerability

See section 2.2 for a more complete explanation of these terms. Mitigation measures reduce the exposure or the vulnerability to the hazard. The reduction in risk is then a measure of the effectiveness of mitigation.

The purpose of this report is to quantitatively estimate the tsunami hazard around the New Zealand coast, so the results may be applied to the estimation of risk and to the development of appropriate mitigation measures.

6.2 METHODOLOGY OUTLINE

The approach used for estimating tsunami hazard in this report is based on a Monte-Carlo modelling process. The method aims to estimate the maximum tsunami height that can be expected over a specified interval of time within sections of the New Zealand coast that are approximately 20 km long. As is the case in most areas of science, an estimate of tsunami hazard is of little value without an assessment of the uncertainty in that estimate, and consequently the estimation of uncertainties plays a major role in the methods used for this report.

To understand the methodology, it is first useful to clearly distinguish between variability and uncertainty. Variability refers to the natural variations that occur between different events. For instance the magnitude of earthquakes on a fault naturally varies from one earthquake to the next. Uncertainty, on the other hand, is a measure of our lack of knowledge about things which are constant in time. For example while the shape of a fault is fixed (at least within the timeframes we are interested in), its shape is not known exactly, and the uncertainty is a measure of how well it is known.

Our Monte-Carlo analysis operates on two levels (Figure 6.1). On the inner level we assume that we have perfect knowledge of the uncertain parameters that do not vary over time, and carry out a hazard assessment using Monte-Carlo sampling of those properties that naturally vary between events. On the outer level we perform Monte-Carlo sampling of the uncertain parameters, and use this to build up a set of hazard estimates that differ from those calculated for the inner level. The spread of these estimates represents the uncertainty in the hazard.

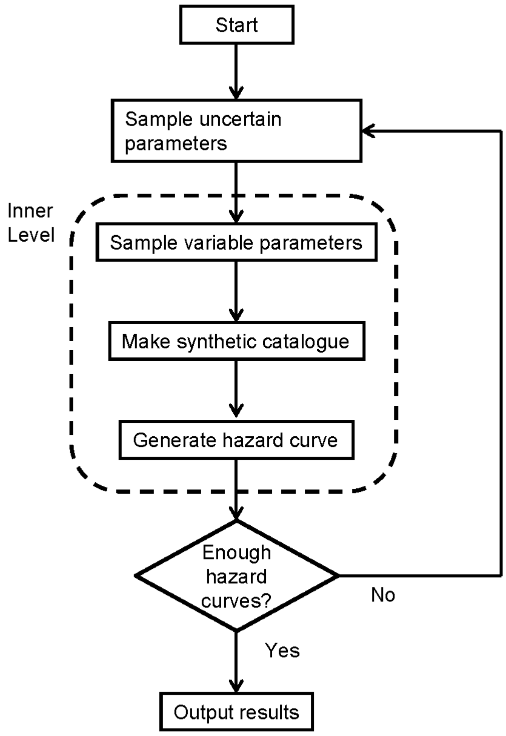

Figure 6.1 Simplified flow-chart representation of the Monte-Carlo modelling scheme.

A more detailed representation of the method is shown in Figure 6.2; in this figure each row going across the chart describes the steps used to construct one tsunami hazard curve. These steps are repeated many times using different samples of the uncertain parameters, and from these it is possible to assign 'error bars' to the tsunami hazard curves.

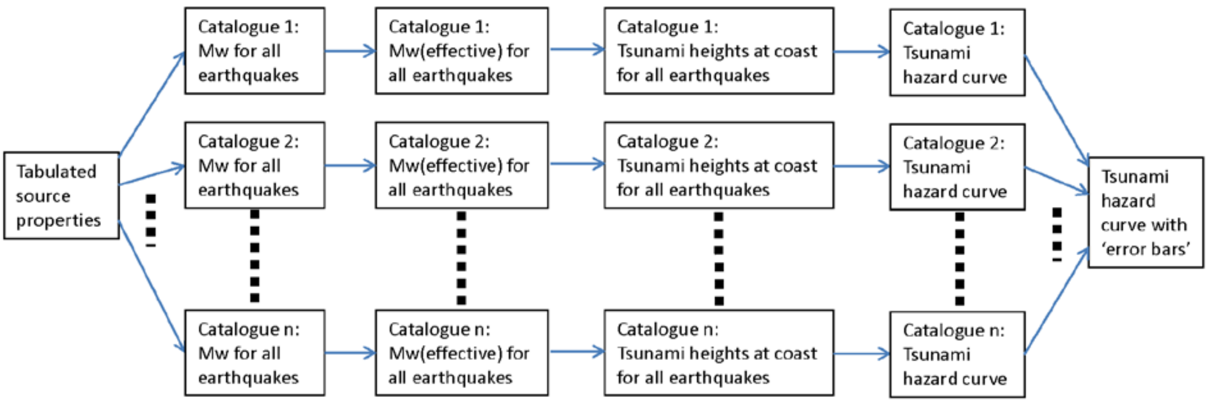

Figure 6.2 Representation of the Monte-Carlo modelling scheme.

Each hazard curve describes the maximum tsunami height reached within a coastal section, as a function of return period (see Section 6.6 and Appendix 7.4 for more details). By sampling from the uncertain parameters, and creating multiple hazard curves, it is possible to estimate the uncertainty in the tsunami hazard (Figure 6.3).

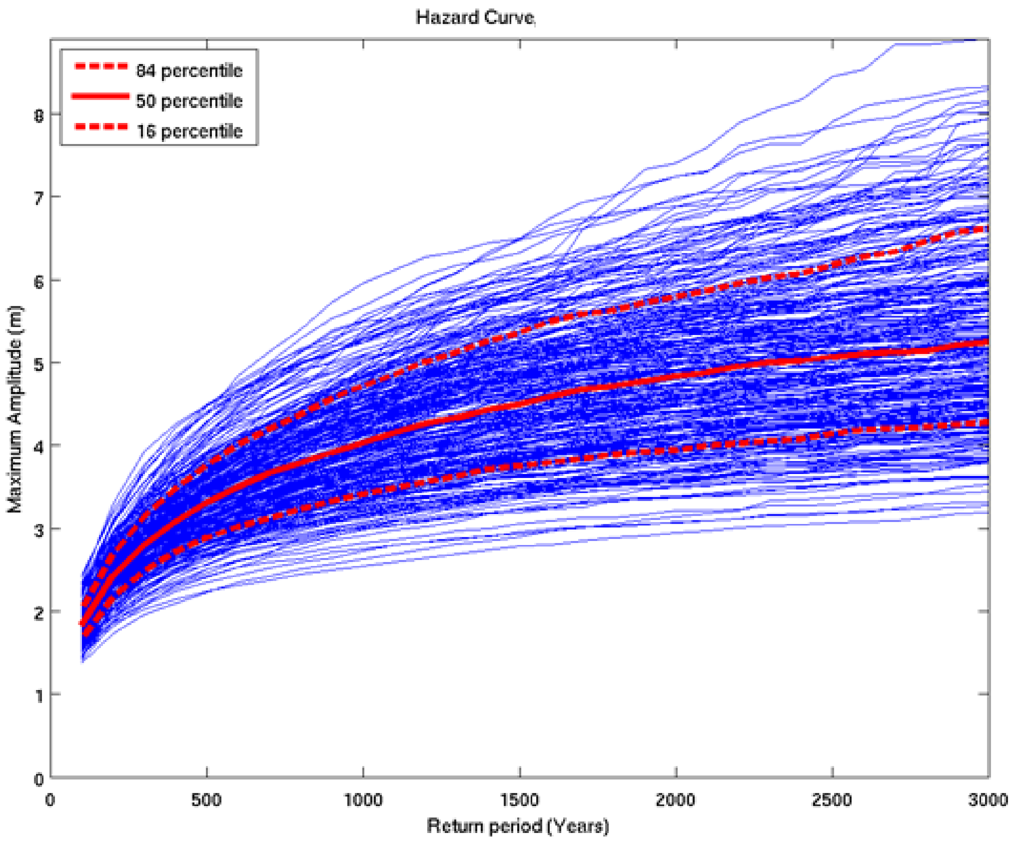

Figure 6.3 Hazard curves for 300 samples of the uncertain parameters, illustrating how the 16th, 50th and 84th percentiles of uncertainty are calculated for one coastal section.

6.3 TYPES OF UNCERTAINTY AND VARIABILITY

The uncertainties and variabilities fall into two broad categories—those associated with the source earthquake, and those associated with the modelling process. For earthquakes, the primary uncertainty is the true form of the magnitude-frequency distribution of the faults (i.e., knowing how often earthquakes of varying magnitude occur along a fault), though it also encompasses such things as uncertainty in the geometry of the faults. The earthquake variabilities represent the variation in magnitude from event to event on a particular fault, and also the variation in the distribution of slip (even among earthquakes of the same magnitude). Modelling uncertainty, on the other hand, reflects the inability of the model to fully capture the physics of tsunami generation and propagation, and uncertainties in bathymetric data. A table summarising the different types of uncertainty and variability, with pointers for further information, is presented in Appendix 7.1.

6.4 SOURCE DEFINITION

An essential input to our probabilistic hazard model is a definition of the physical and statistical properties of the various tsunami sources.

The scope of this report is to define the tsunami hazard within timeframes of up to 2500 years. On these timescales the major contribution to tsunami hazard comes from both distant and local earthquakes, and these are the sources considered here (See 'Tsunami Sources' Chapter 5). For some regions of the country, submarine landslides may contribute to the tsunami hazard in these timeframes as well, and initial steps towards estimating potential landslide contributions are described in Appendix 6.

The definition of tsunami sources from subduction-zone earthquakes, which constitute all distant earthquake sources and the most important local ones, drew heavily on work that has been done for the Global Earthquake Model (GEM). The assumed parameters for subduction-zone earthquakes used for this report are shown in Appendix 3.

The starting point for defining tsunami sources for local non-subduction zone earthquakes was the New Zealand Seismic Hazard Model (NZSHM; Stirling et al., 2012). The faults in the seismic hazard model were filtered to exclude those with characteristic magnitudes below 6.5 (which are too small to generate enough displacement to cause a tsunami), those with strike-slip mechanisms, and those that are entirely on-shore. The remaining faults are summarised in Appendix 4. Additional fault sources were added in the Outer Rise, the Taranaki Basin, and along the west coast of the South Island; these fault sources are only tentatively identified in geophysical data, and are summarised in Appendix 5.

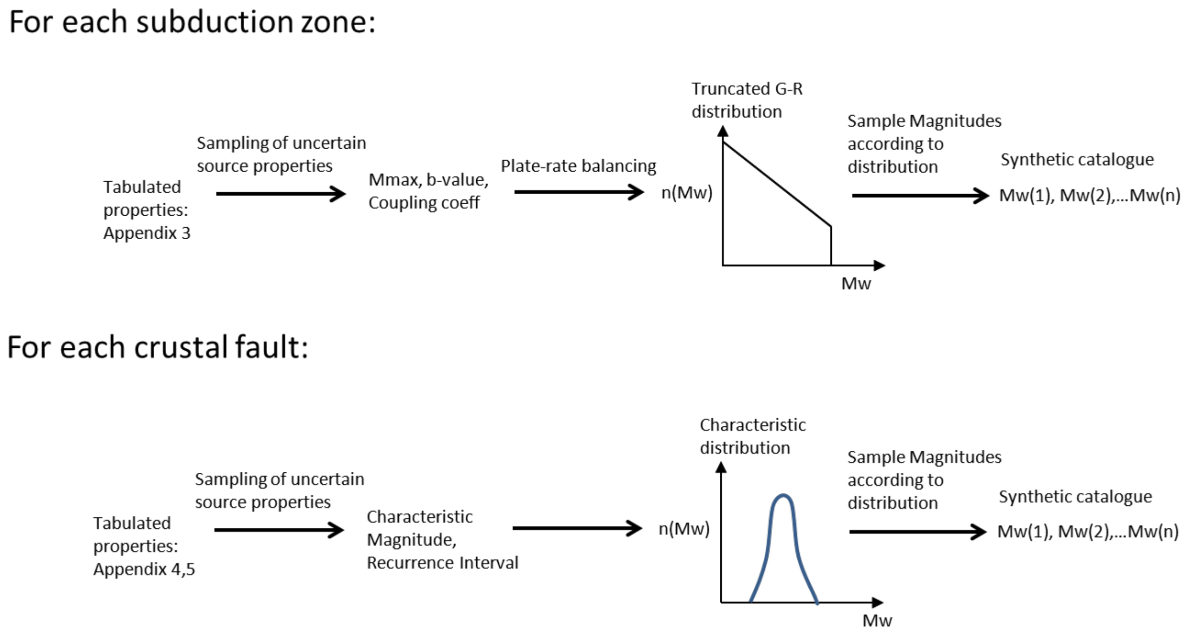

Figure 6.4 Illustration of the steps by which the tabulated fault properties are used to create synthetic earthquake catalogues. This process corresponds to the leftmost set of arrows in Figure 6.2.

The creation of synthetic earthquake catalogues from the tabulated fault and subduction zone properties is illustrated in Figure 6.4. Additional details regarding the construction of the synthetic catalogues are presented in Appendix 7.2.

6.5 TREATMENT OF VARIABLE SLIP AND MODELLING UNCERTAINTY

Magnitude alone is not enough to determine the size of tsunami that will be produced by an earthquake. It has been shown that the distribution of slip on a fault also plays an important role. Geist (2002) found that the peak amplitude of nearshore tsunami varied by over a factor of 3 depending on the slip distribution. Preliminary work by Mueller et al. (2012) has demonstrated great variation in the extent of inundation as a result of variable slip. It was found that in order to encompass the union of the inundation from 60 variable slip models of a M_W 8.4 earthquake (i.e., the area of land inundated in at least one of the 60 models), a uniform slip model would need to be of M_W 8.9 (a difference of 0.5 magnitude units). This suggests that locally the effect of variable slip may be approximately equivalent to a change in the effective magnitude of the event.

Within our model we treat the effect of non-uniform slip as if it has the effect of altering the effective magnitude of the earthquake. By adding a normally distributed variation to the magnitudes in the synthetic earthquake catalogue, we create a new catalogue of ‘effective magnitudes’ that represent the consequences of the variable slip. It may be argued that this is not a true representation of the effects of variable slip, since variable slip may enhance the tsunami at some locations while reducing it at others, whereas our approach sees the effective magnitude of the earthquake increase (or decrease) in the same way at all locations. This would be a problem if we were to look at correlated hazards across multiple locations, however as long as we view the hazard on a ‘one site at a time’ basis, this approximation appears valid.

This approach, of creating a catalogue of ‘effective magnitudes’, also provides a convenient way to incorporate the effects of modelling uncertainties. We regard the effects of modelling approximations and of limited data on source geometry and ocean bathymetry, as having a similar effect to (usually small) increases or decreases in the magnitude of the source earthquake. Table 6.1 summarises the parameters used for this purpose:

Table 6.1 Standard deviations associated with random adjustments to the synthetic catalogue to create a catalogue of ‘effective magnitudes’. The fault-specific uncertainty covers uncertainties that are specific to the modelling of each fault, while the method bias covers uncertainties that cause a systematic bias across all faults. Units are in the M_W scale.

	Local Crust Fault (empirical model)	**Local Subduction Zone (numerical model)**	**Distant Subduction Zone (numerical model)**
Variability (e.g. non-uniform slip): σ_v	0.25	0.25	0.1
Modelling uncertainty (fault specific): σ_u	0.2	0.1	0.1
Modelling uncertainty (method bias): σ_b	0.14	0.05	0.05

An ‘effective magnitude’ is calculated by applying the parameters that describe the uncertainties and variabilities that affect tsunami heights, using the following equation:

$$Mw_{ijk}(effective) = Mw_{ijk} + \sigma_v N(0,1)_{ijk} + \sigma_u N(0,1)_{jk} + \sigma_b N(0,1)_k \qquad \textbf{Equation 6.1}$$

where i represents individual earthquakes on fault j, described in synthetic catalogue k. N(0,1) represents a number sampled from the normal distribution with a mean of zero and a standard deviation of 1. The subscript to N(0,1) describes the set over which individual samples are made, e.g., $N(0,1)_{jk}$ is sampled for each fault in each catalogue, but has the same value for all earthquakes on a particular fault in a particular catalogue. This calculation of an ‘effective magnitude’ corresponds to the second step (going left to right) in Figure 6.2.

The reasoning behind the choice of values for the parameters in Table 6.1 is explained in Appendix 7.3.

6.6 ESTIMATION OF TSUNAMI HEIGHTS

The Monte-Carlo method requires us to estimate the maximum tsunami height for each section of the coast following every event in a synthetic catalogue of earthquakes. Various techniques can be used to estimate the tsunami heights, but it is important that the calculation can be performed quickly, since it is necessary to model many events to produce robust statistics.

Three different methods are used here:

- Finding the closest available model (in terms of location and magnitude) in a pre-computed catalogue, and then applying scaling to the model results to match the synthetic catalogue magnitude.
- Using a collection of pre-calculated models of tsunami from a particular source region to estimate coefficients in a semi-empirical scaling relationship.
- Using an empirically-determined scaling-relationship based only on the magnitude and distance of historical earthquakes that have caused tsunami.

Broadly speaking, the quality of results diminishes down this list of methods, as does the work required to implement them for any particular source. The first method has been applied to subduction zone sources close to New Zealand, specifically the Hikurangi, Kermadec and Puysegur Trenches, where the location of the earthquake within the source region plays a very major role in determining the consequences for particular sections of the New Zealand coast (see Appendix 7.4 for more details). The second method has been applied to all other Pacific subduction zones, i.e., those at regional or distant locations from New Zealand; the tsunami consequences of earthquakes at these distances are less sensitive to the precise location of the source. This method uses the empirical approach of Abe (1979), except that numerical results from the New Zealand forecast database were used instead of historical catalogue data (see Appendix 7.4 and Section 4.5.1.1 for more details). The third method applies the empirical modelling approach developed by Abe (1995), and is applied to estimating the tsunami caused by local faults other than the subduction zones (see Appendix 7.4 and Section 4.5.1.2 for more details).

Tsunami height is defined here as the maximum height that the tsunami would reach against an imaginary vertical wall at the coast, relative to the background sea level at the time of the tsunami. This choice of criteria permits us to re-use the modelling used for the New Zealand forecast database. In many situations where the tsunami does not penetrate far inland (i.e., less than several kilometres) this represents a reasonable approximation to the expected run-up height, although in a small number of locations where a tsunami is focussed by small-scale topographic features, the run-up may locally reach up to about twice this height. For most practical mitigation measures it is expected that the tsunami heights derived from this study will not be used directly, but will be deaggregated (see Section 6.8) to determine the extent to which different sources contribute to the hazard, and this will be used to decide upon specific scenarios for detailed inundation modelling.

In the case of the empirical equation used for local crustal faults, Abe (1995) relates the predicted tsunami height to the average run-up height measurement, rather than to the maximum height against an imaginary vertical wall at the shore[20]. We have treated these two quantities as being equivalent, but there is considerable uncertainty about this relationship; this uncertainty contributes to the corresponding bias parameter in Table 6.1.

The numerical models used for this study were developed using the COMCOT code (Wang and Liu, 2006; Wang and Liu, 2007). A series of nested bathymetric grids were developed, ranging in size from the entire Pacific Ocean to small regions of New Zealand. Models from the New Zealand tsunami forecast database were used for the distant subduction zone sources. The local subduction zones were modelled using the same nested grid configuration in order to maintain consistency. In this grid setup the non-linear shallow water wave equations were used to model the grids closest to New Zealand, where the water depths are such that the non-linear effects may be significant, and the linear shallow water equations were used for all of the outer grids.

6.7 CALCULATION

The Monte-Carlo analysis of epistemic uncertainty was made using 300 samples of the uncertain parameters. For each of these 300 samples a 100,000 year synthetic catalogue of earthquakes was constructed. Re-running the analysis using these same parameters and a different set of random numbers demonstrated good repeatability of the results, with variations in the hazard curves that were small compared to the cumulative effect of other sources of uncertainty. The probabilistic tsunami hazard model in this report does not include modelling of tides.

6.8 DEAGGREGATION OF TSUNAMI SOURCES

The process described in the preceding sections allows the construction of tsunami hazard curves for individual sections of coast. These curves, which will be described in detail in section 6.9, indicate the height of tsunami that may be expected in a given time frame. On their own these curves do not provide a measure of the extent of inundation, only the maximum height at the coast.

Deaggregation is a process for establishing the extent to which different tsunami sources contribute to the probabilistic tsunami hazard. The main purpose for the deaggregation used in this report is to establish a particular set of scenarios whose inundation can be modelled to give an approximation of the onshore tsunami hazard at a particular level of probability (i.e., return period) and confidence.

The probabilistic hazard analysis described in Sections 6.2 to 6.7 involves the generation of a large number N (typically 300) of synthetic catalogues of effective earthquake magnitude. Each catalogue represents a sequence of earthquakes generated assuming a particular sampling of the uncertain parameters. For a selected return period R (500 years and 2500 years have been used) the median tsunami height H(R) was found from the corresponding hazard curve for the site of interest. Each synthetic catalogue was searched to find the three

[20] In earlier work Abe (1981; 1985) calibrated the tsunami height in his empirical equations using the amplitudes measured by tide gauges, however it was shown that the Japanese tide gauges of this era were often likely to underestimate tsunami amplitude because of slow instrument response (Satake et al., 1988), so we regard this interpretation as unreliable.

earthquakes that produced tsunamis at the site which were closest in height to H(R). The proportion of these 3xN events coming from particular faults was calculated, and this was used to generate the pie charts described in section 6.9. In addition, an estimate was made of the median effective magnitude of the selected earthquakes from each of the identified faults.

This deaggregation procedure can probably be improved upon with further research. In particular it may not be ideal for use in situations involving both long return periods and high levels of confidence (e.g., 2500 year RP and 95% confidence) as it is possible that some catalogues may not then contain events that reach the H(R) of a given coastal section.

6.9 RESULTS

The coast of New Zealand was divided into 268 sections, each approximately 20 km long as measured along the open coast[21]. Within each section the model produces a hazard curve that illustrates the expected maximum tsunami height (as defined in Section 6.6) as a function of return period. A series of hazard curves for several major cities are shown in Figure 6.2 to Figure 6.33: the solid line indicates the best-estimate hazard curve and the dashed lines are 'error bars' indicating the 16th and 84th percentile of uncertainty. During a tsunami the peak water levels will vary considerably even across a 20 km section of coast; in the curves shown here the 'maximum amplitude' should be interpreted as the tsunami height measured at the location within the section where it is highest; the median tsunami height within the section may be significantly lower (see, e.g., Power et al., 2010).

Opposite the hazard curves are two pie charts; these show the breakdown of the relative contribution of different fault sources to the median hazard (i.e., the 50th percentile of uncertainty in the hazard curves) at 500 years and 2500 years. The area of each slice of the pie indicates the proportion of the hazard for which a particular fault is responsible—the larger the area the more frequently that source is expected to produce tsunami of the size corresponding to the return period.

The pie charts indicate the six tsunami sources that most frequently generate tsunami at the median height (in terms of confidence) for the 500 year and 2500 year return periods. The pie charts also show the effective magnitude of earthquakes on these faults that are necessary to generate a tsunami of this height. While these events are estimated to produce tsunami of the same height at the coast, the extent of inundation is expected to vary with the number and period of waves.

In order to make an estimate of the extent of inundation at the 500 year and 2500 year return period, we suggest that the six sources making the greatest contribution are all modelled through to inundation, assuming earthquakes at the effective magnitudes given on the pie charts. The modelling should assume uniform slip at the specified effective magnitude, and if the source is one of the local subduction zone sources (Hikurangi, Kermadec or Puysegur) the earthquake should be assumed to occur on the part of the interface that the site is most sensitive to (usually the nearest). The union of the six inundations (i.e., the area inundated in

[21] This is primarily an open coast tsunami hazard model. While the modelling did include harbours, they may not be well resolved at the resolution used. Hence all coastal sections included ~20 km of open coast.

one or more of the scenarios) can then be used as a conservative approximation[22] to the extent of inundation at the chosen return period.

The fault labels on the pie charts indicate the estimated magnitude that an earthquake on each source would need to be to produce a tsunami that would reach this height according to our deaggregation. The labelling convention is as follows: first there is a code indicating the general source region (NZ=New Zealand, AK=Alaska, CA=Central America, CD=Cascadia, CL=Chile, CO=Colombia, JP=Japan, MX=Mexico, PE=Peru, PH=Philippines, PNG=Papua New Guinea, SPAC=South Pacific); then comes the fault or subduction zone name (see Appendices 3 and 4); followed by the magnitude from the deaggregation. Sometimes the effective magnitudes may be greater than those considered possible for the fault—this is a consequence of our approximations used to represent the effects of non-uniform slip and other uncertainties. In other words, a uniform slip event of this magnitude is used to approximate a non-uniform slip earthquake of lower magnitude.

In order to compare the hazard at different sites, the hazard at various return periods can be illustrated in a map view. Examples of these maps for return periods of 100, 500 and 2500 years are shown in Figure 6.34 to Figure 6.36.

[22] Tsunami of the same height at the coast will still differ in the extent of inundation as a consequence of other properties such as the number and duration of waves; this is why taking the union of the six inundations is a conservative approximation. It may be possible to remove this bias by using a combination of the individual inundations that are weighted according to their relative frequency, further research is needed to see if this is feasible.

Auckland East Coast

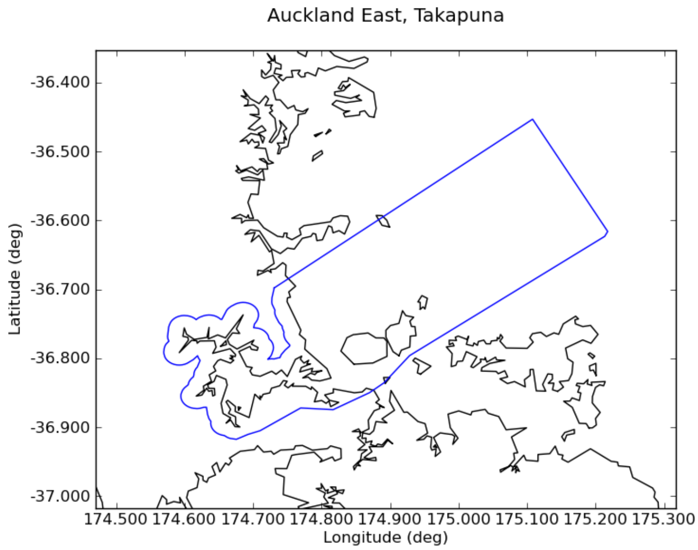

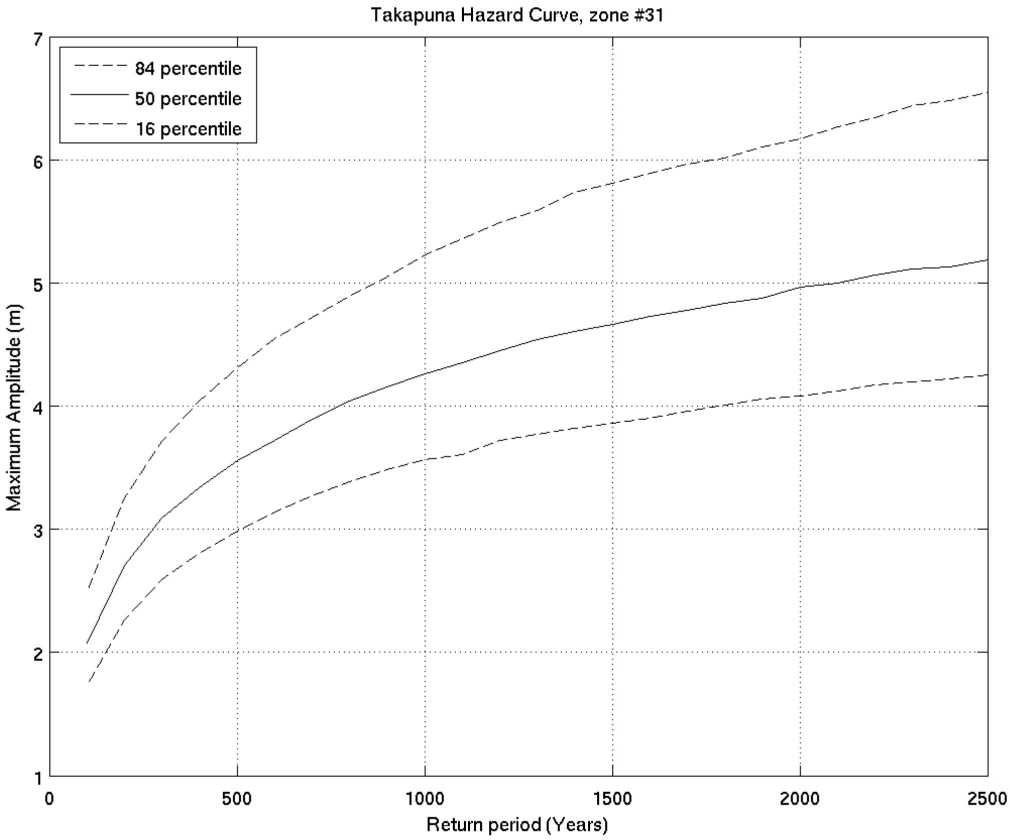

Figure 6.5 Area map and tsunami hazard curve for Auckland East.

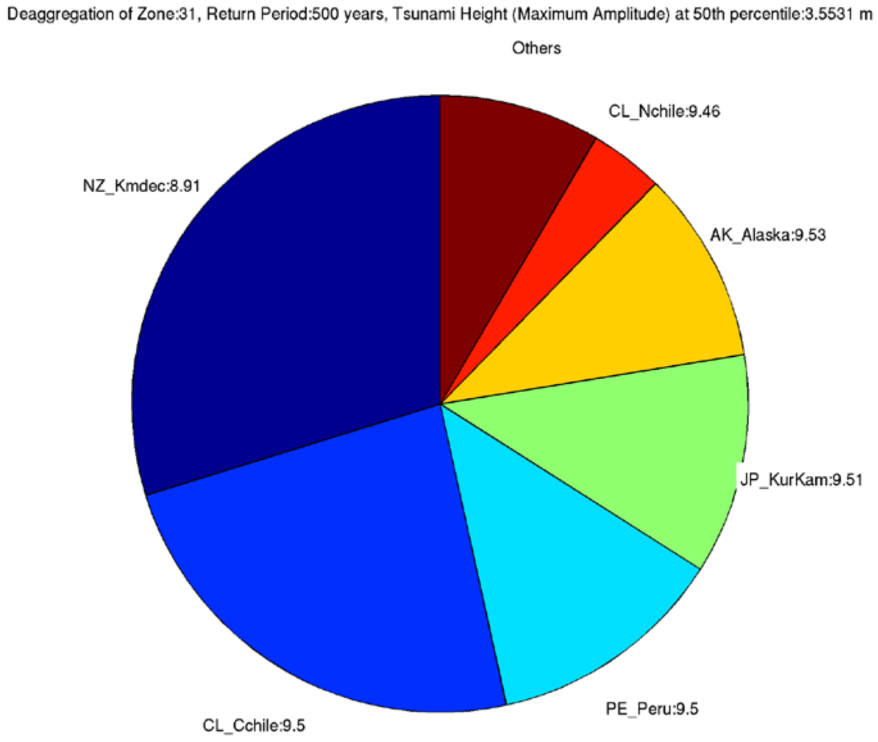

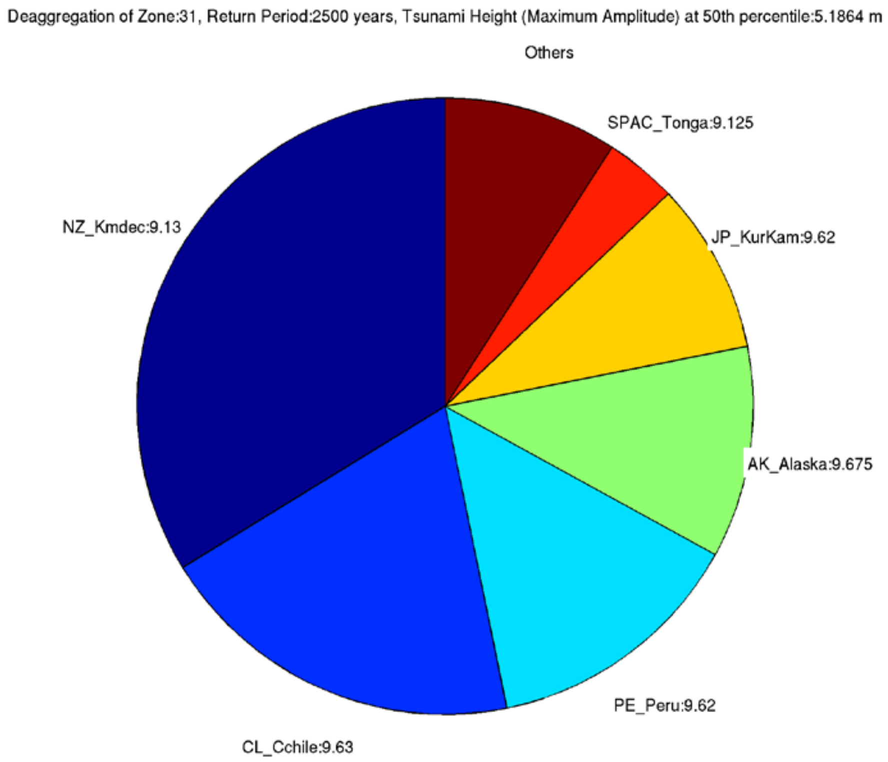

Figure 6.6 Deaggregation of tsunami sources for Auckland East Coast at 500 yr (top) and 2500 yr (bottom) return periods.

Auckland West Coast

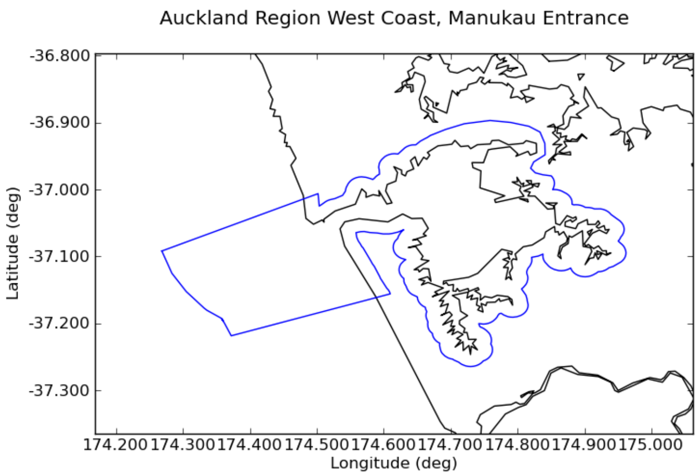

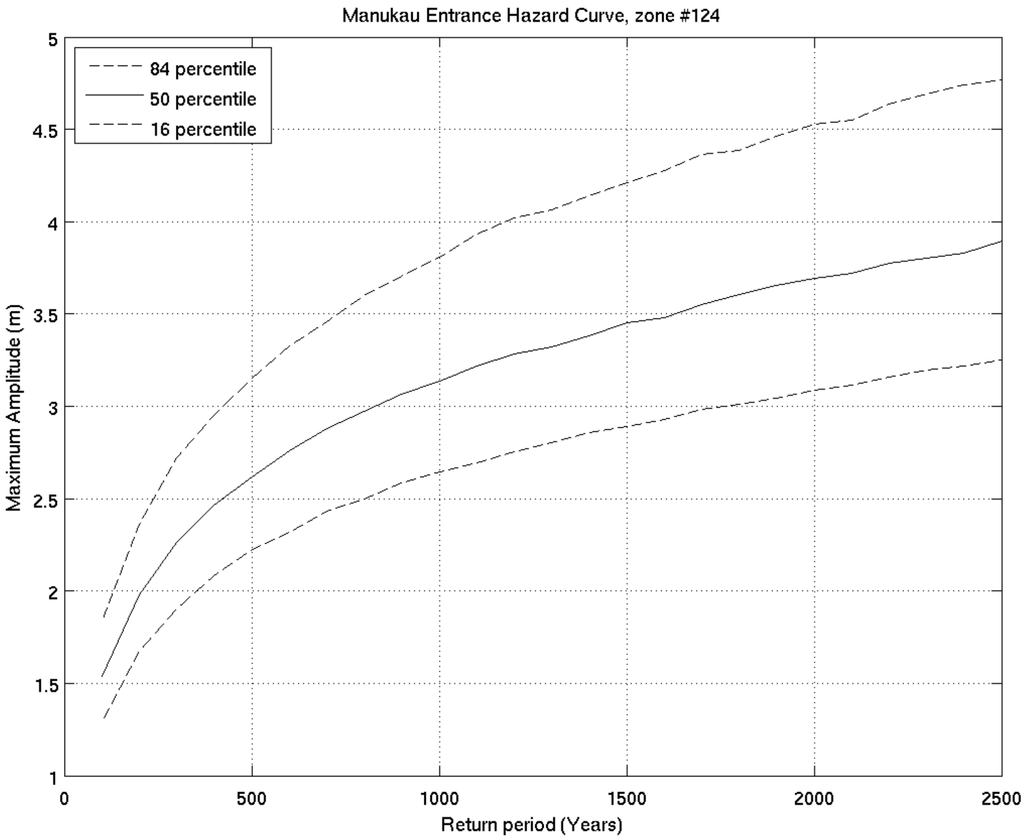

Figure 6.7 Area map and tsunami hazard curve for Auckland West Coast.

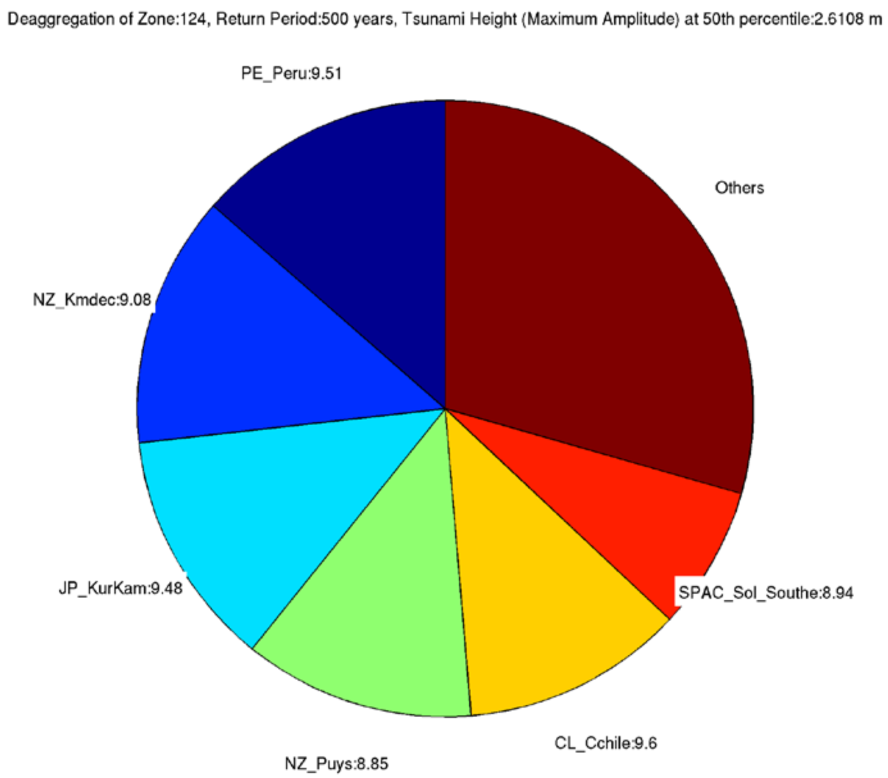

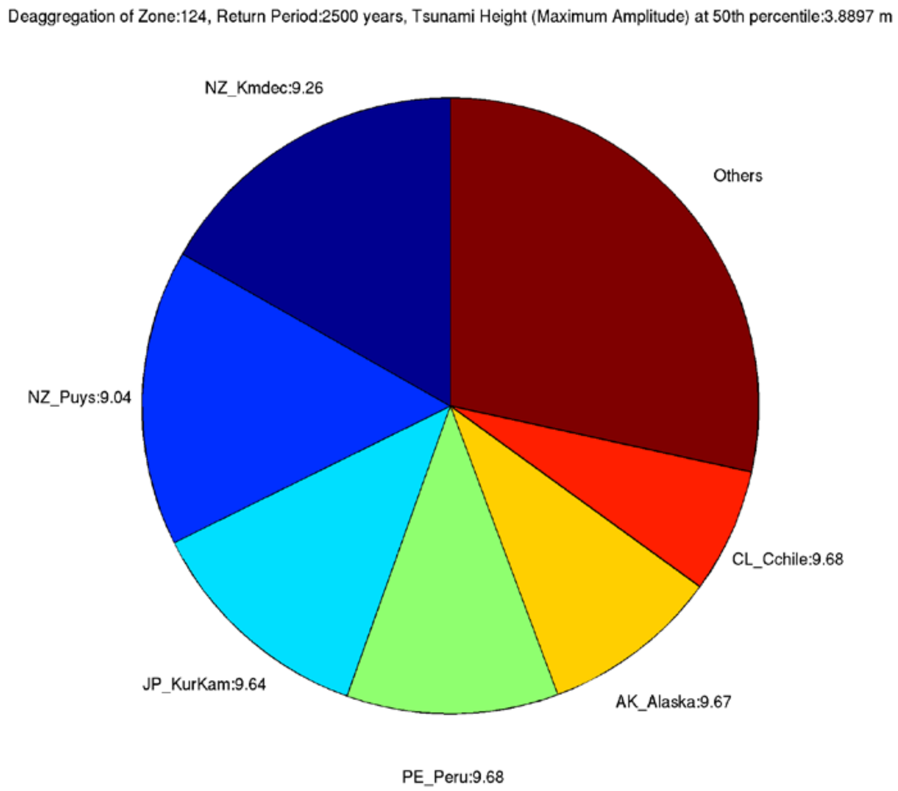

Figure 6.8 Deaggregation of tsunami sources for Auckland West Coast at 500 yr (top) and 2500 yr (bottom) return periods.

Christchurch

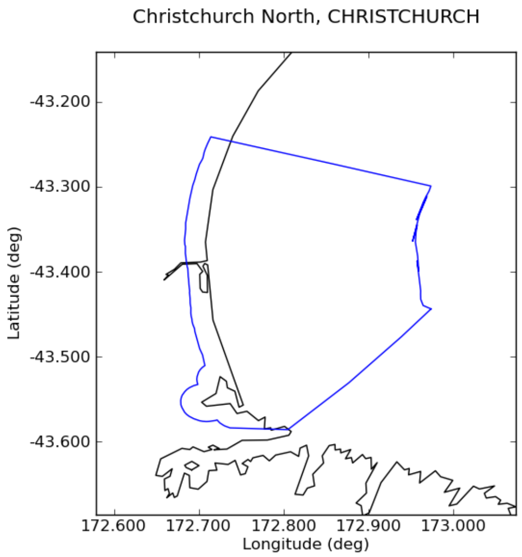

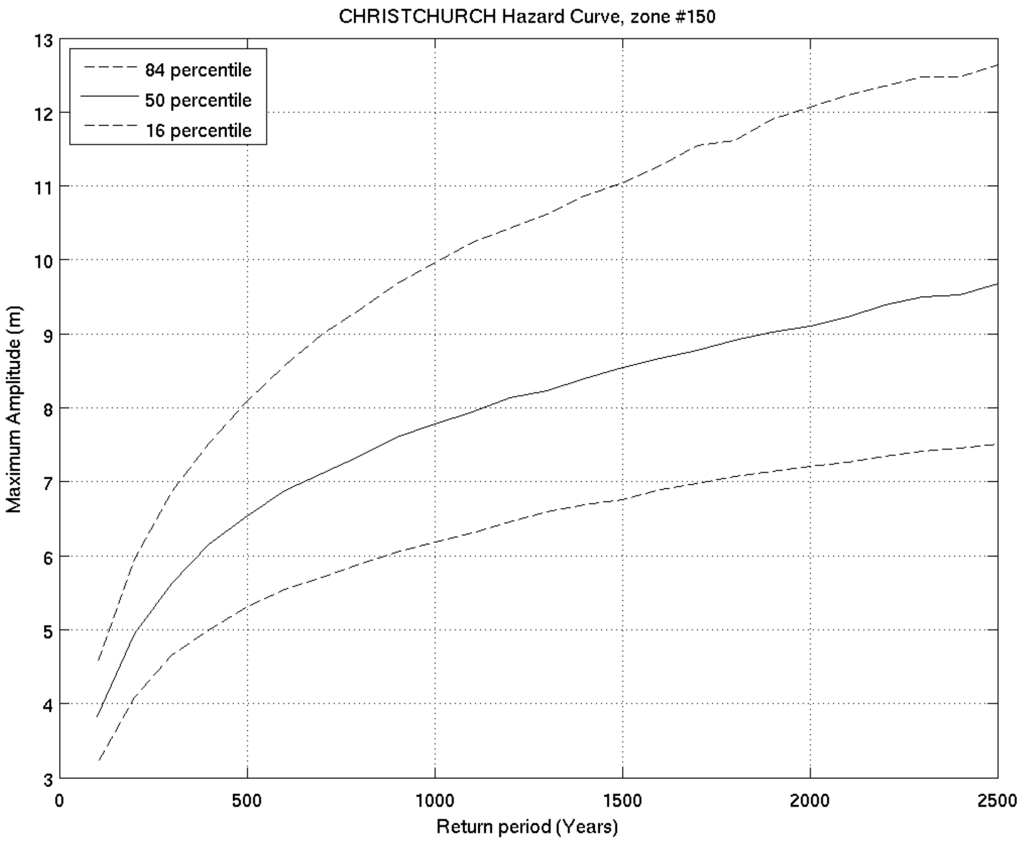

Figure 6.9 Area map and tsunami hazard curve for Christchurch.

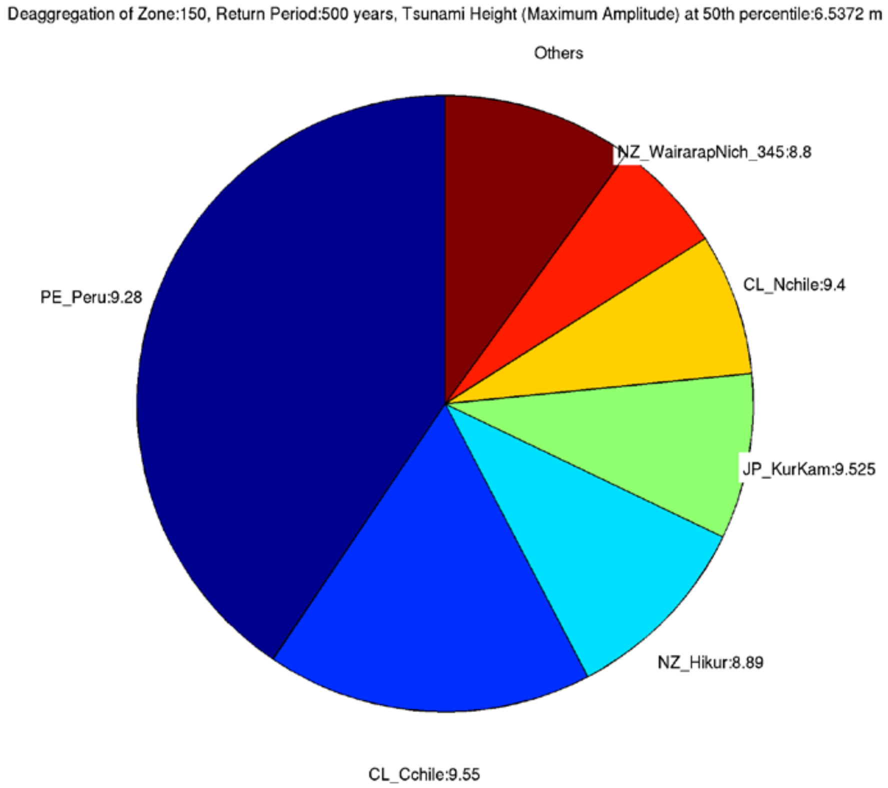

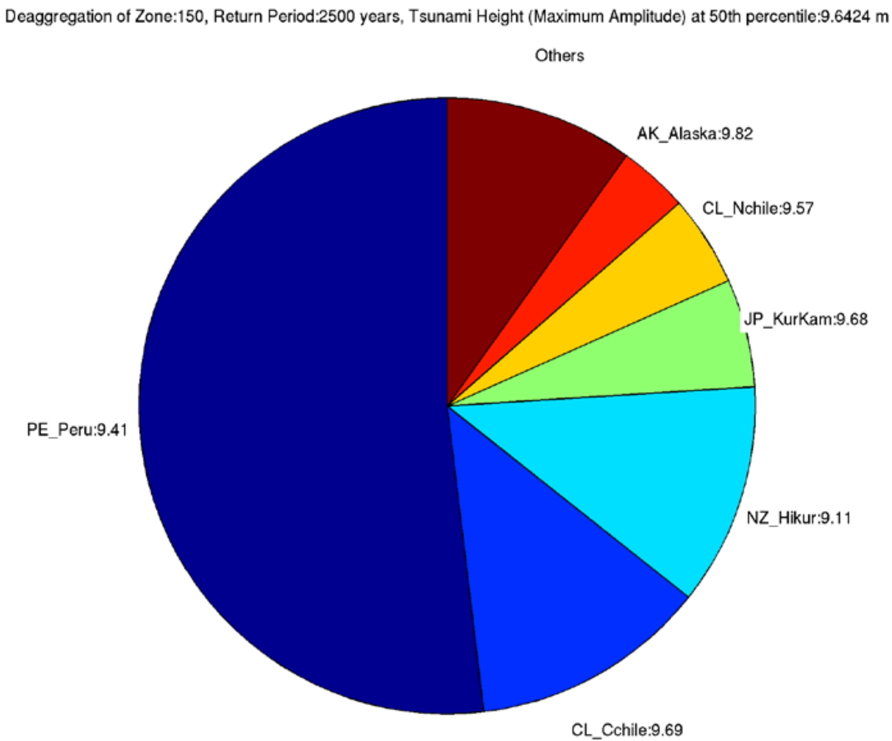

Figure 6.10 Deaggregation of tsunami sources for Christchurch at 500 yr (top) and 2500 yr (bottom) return periods.

Dunedin

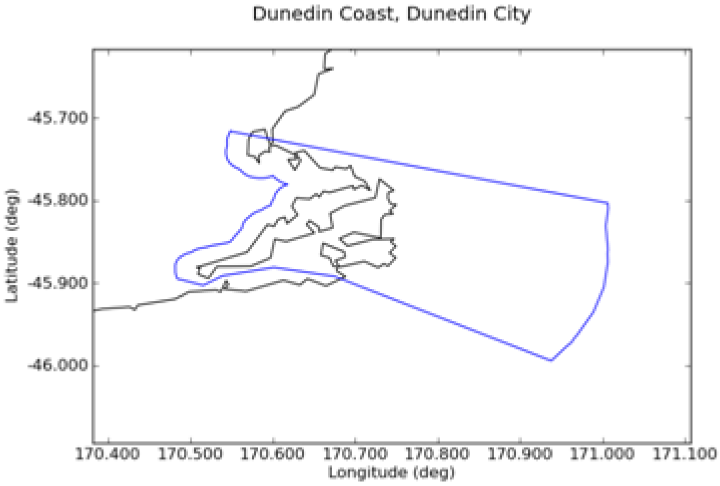

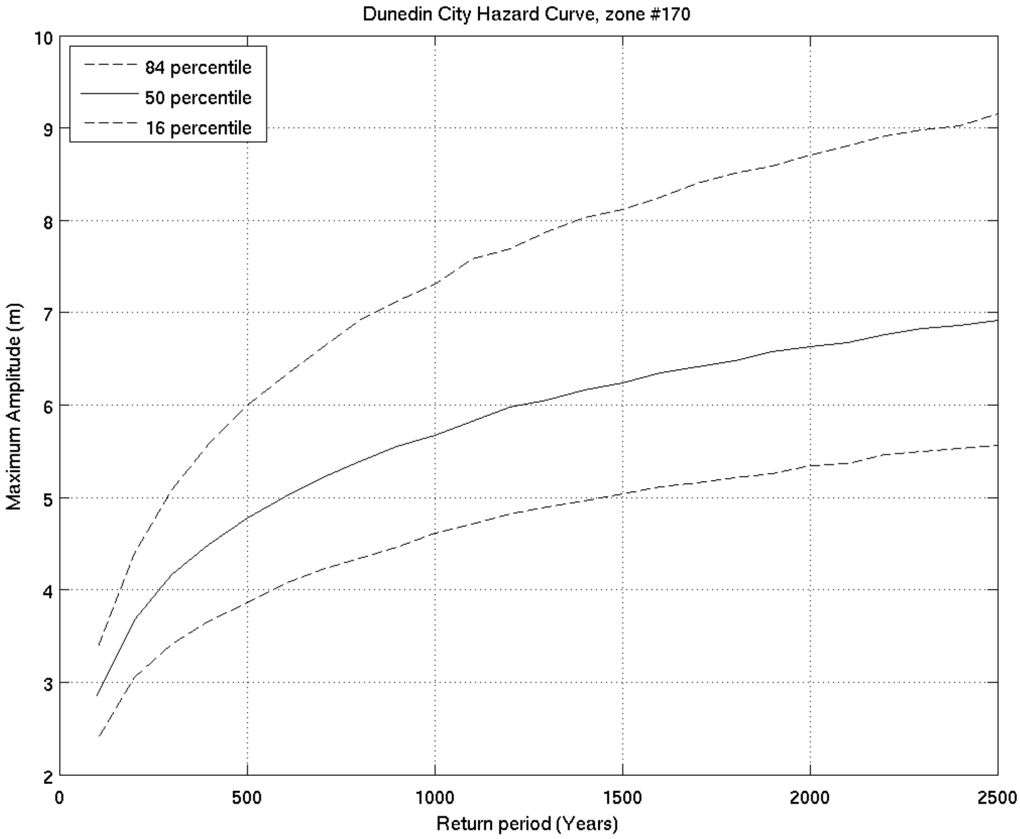

Figure 6.11 Area map and tsunami hazard curve for Dunedin.

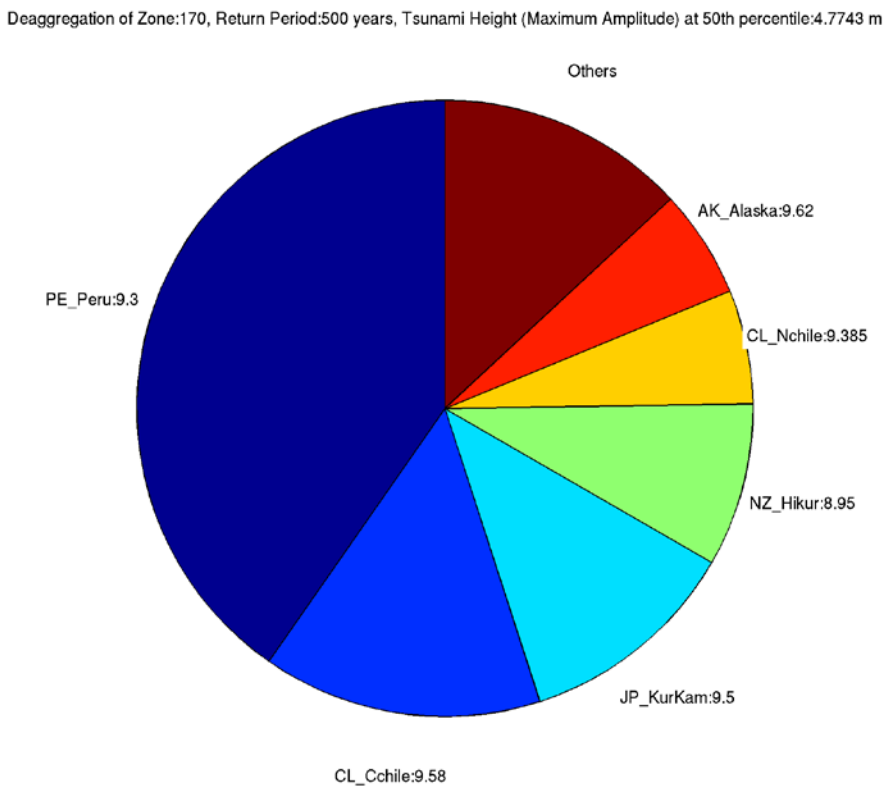

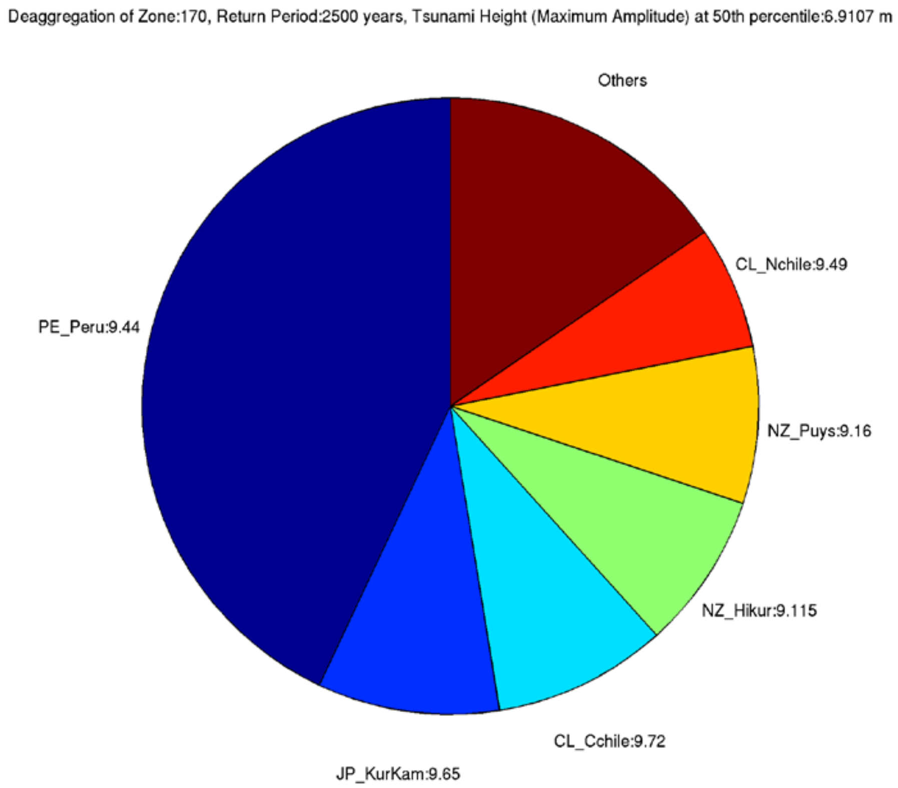

Figure 6.12 Deaggregation of tsunami sources for Dunedin at 500 yr (top) and 2500 yr (bottom) return periods.

Gisborne

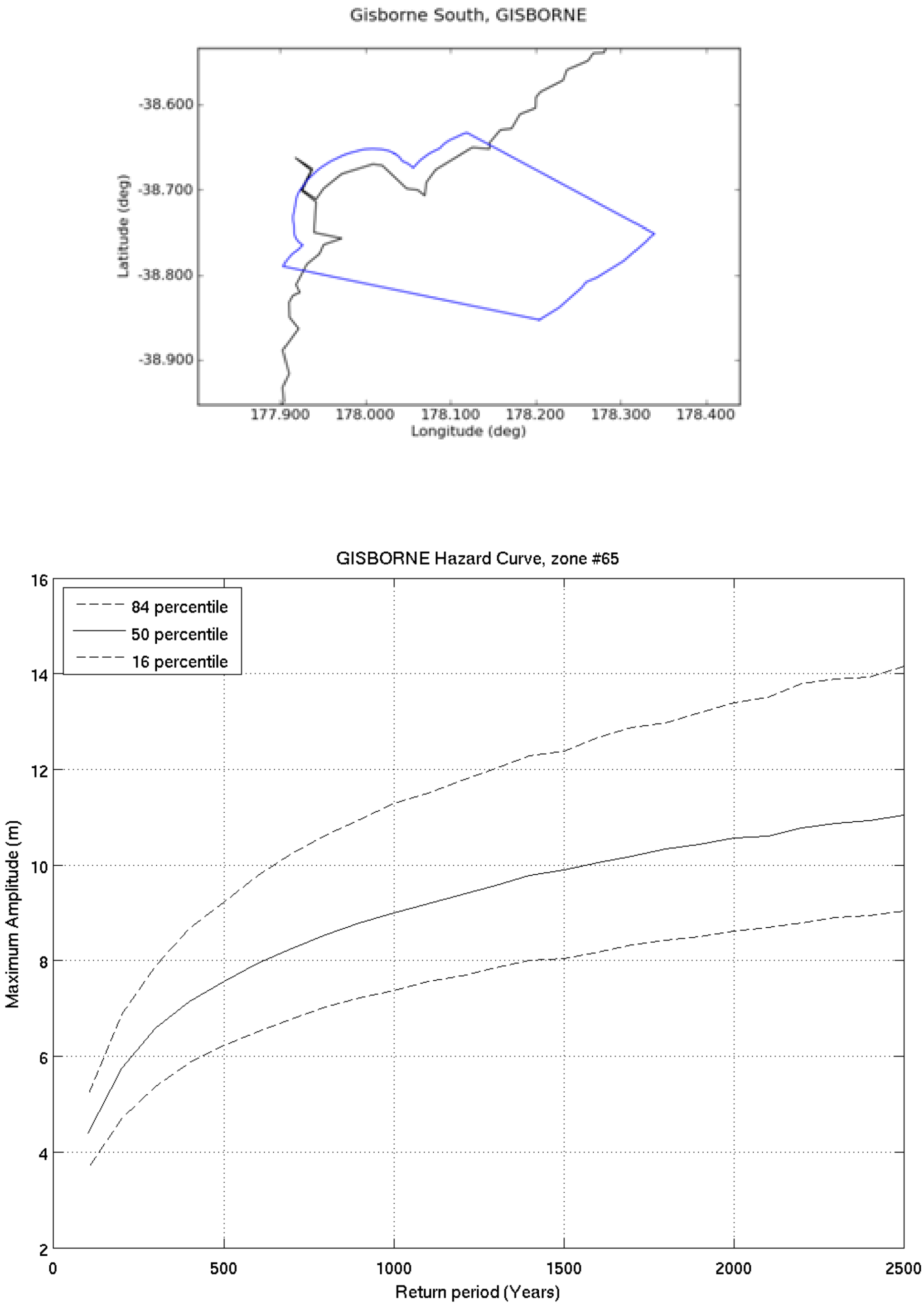

Figure 6.13 Area map and tsunami hazard curve for Gisborne.

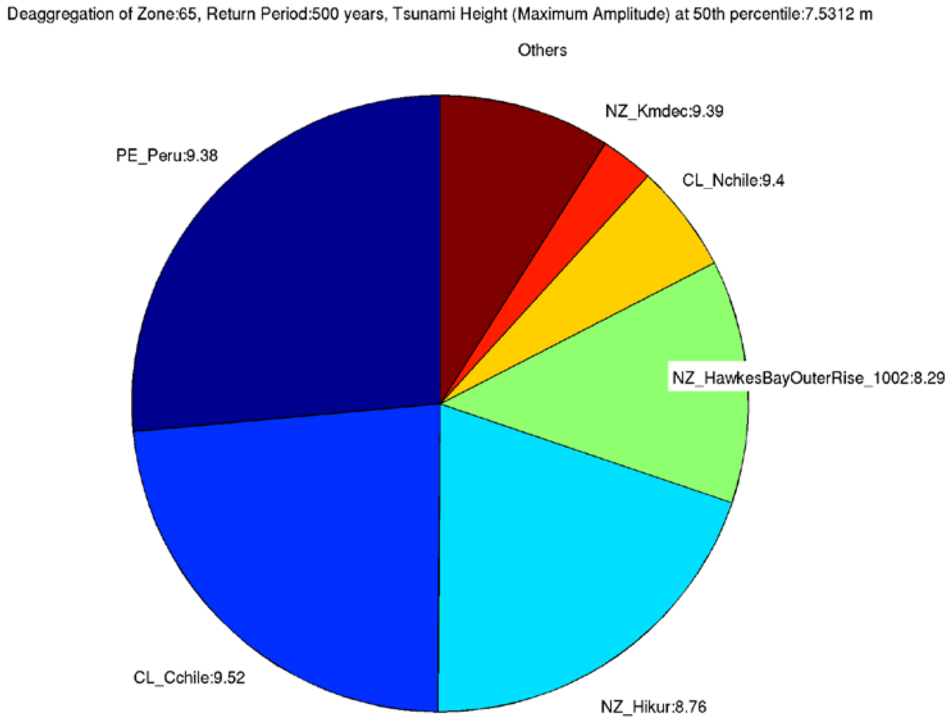

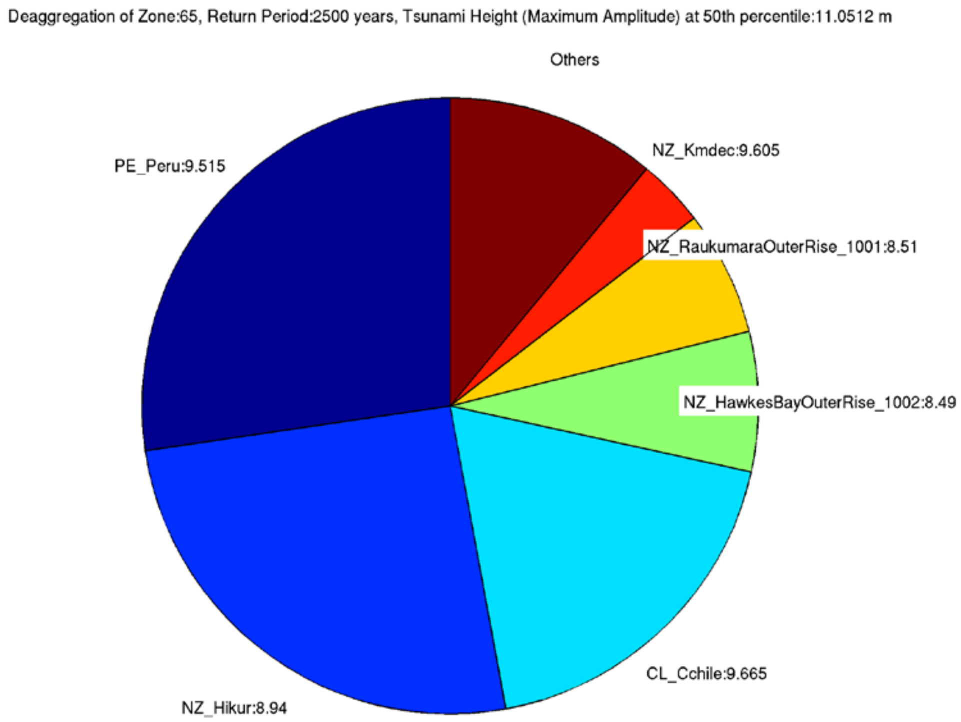

Figure 6.14 Deaggregation of tsunami sources for Gisborne at 500 yr (top) and 2500 yr (bottom) return periods.

Invercargill

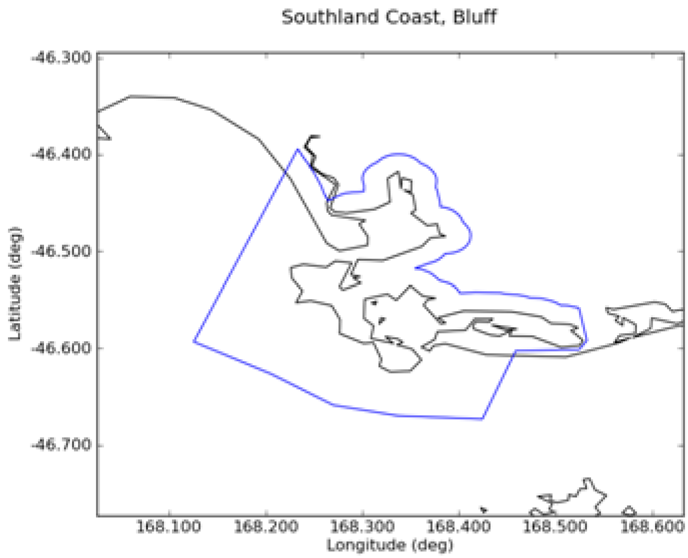

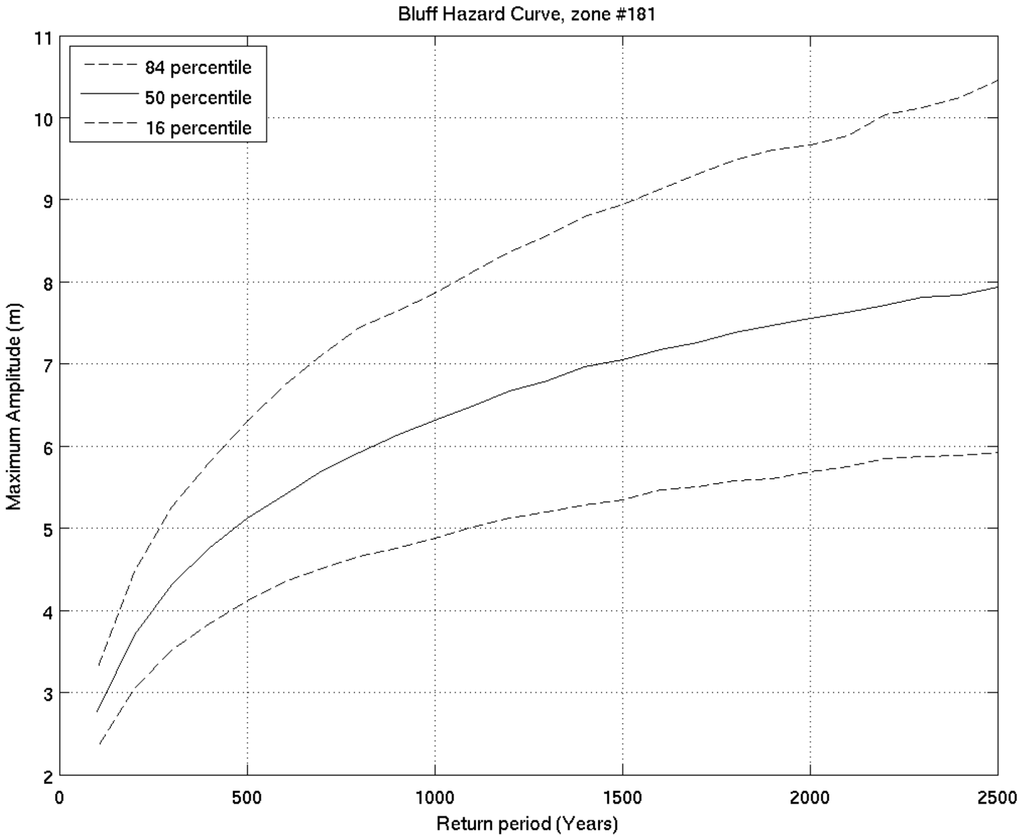

Figure 6.15 Area map and tsunami hazard curve for Invercargill.

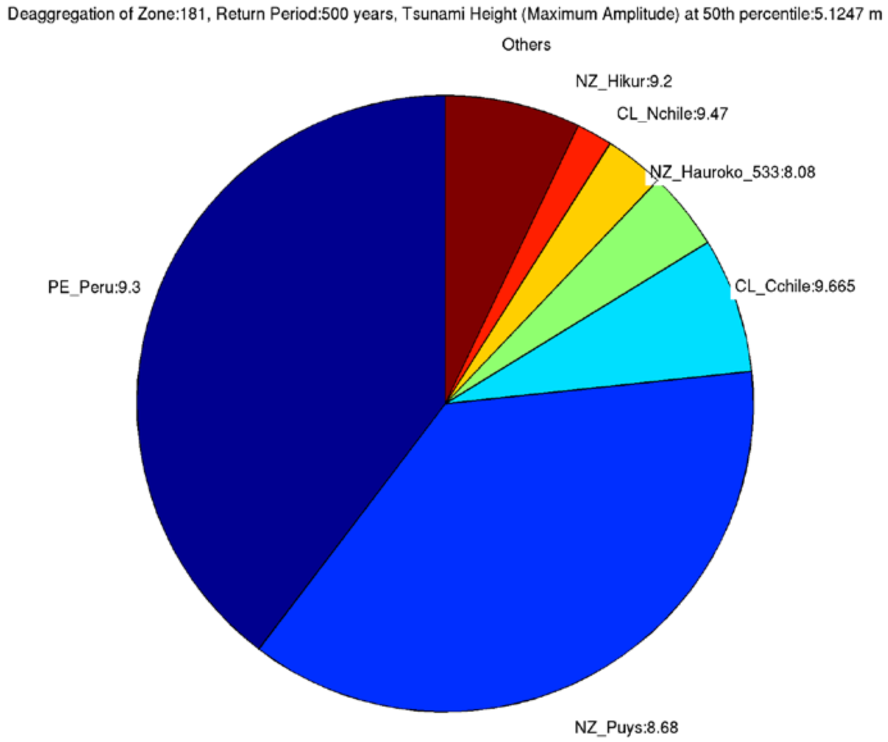

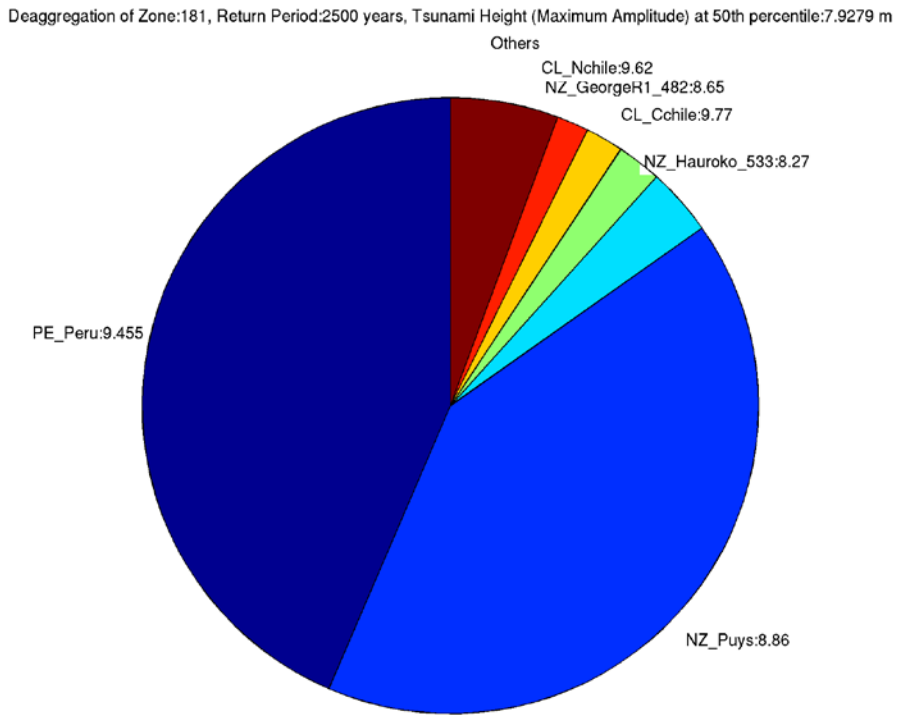

Figure 6.16 Deaggregation of tsunami sources for Invercargill at 500 yr (top) and 2500 yr (bottom) return periods.

Kapiti Coast

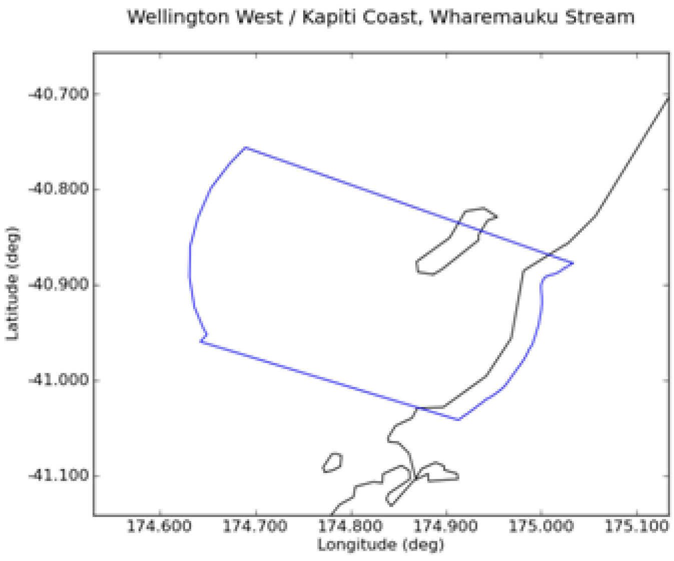

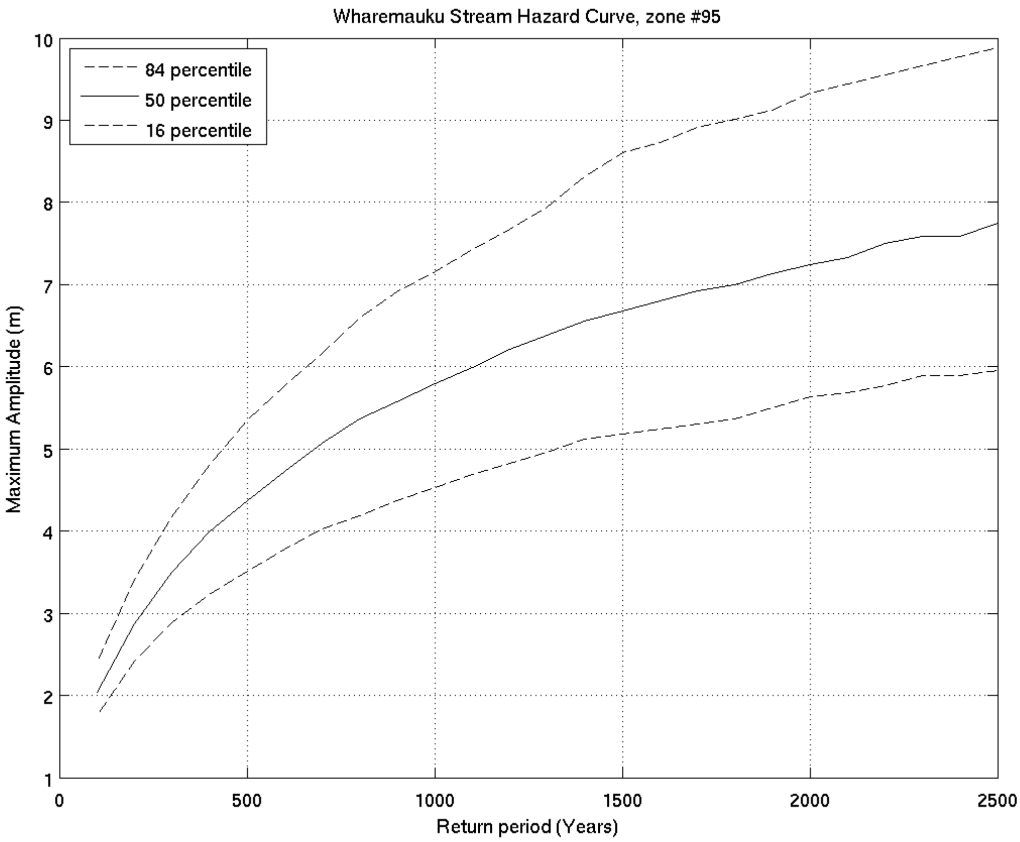

Figure 6.17 Area map and tsunami hazard curve for Kapiti Coast.

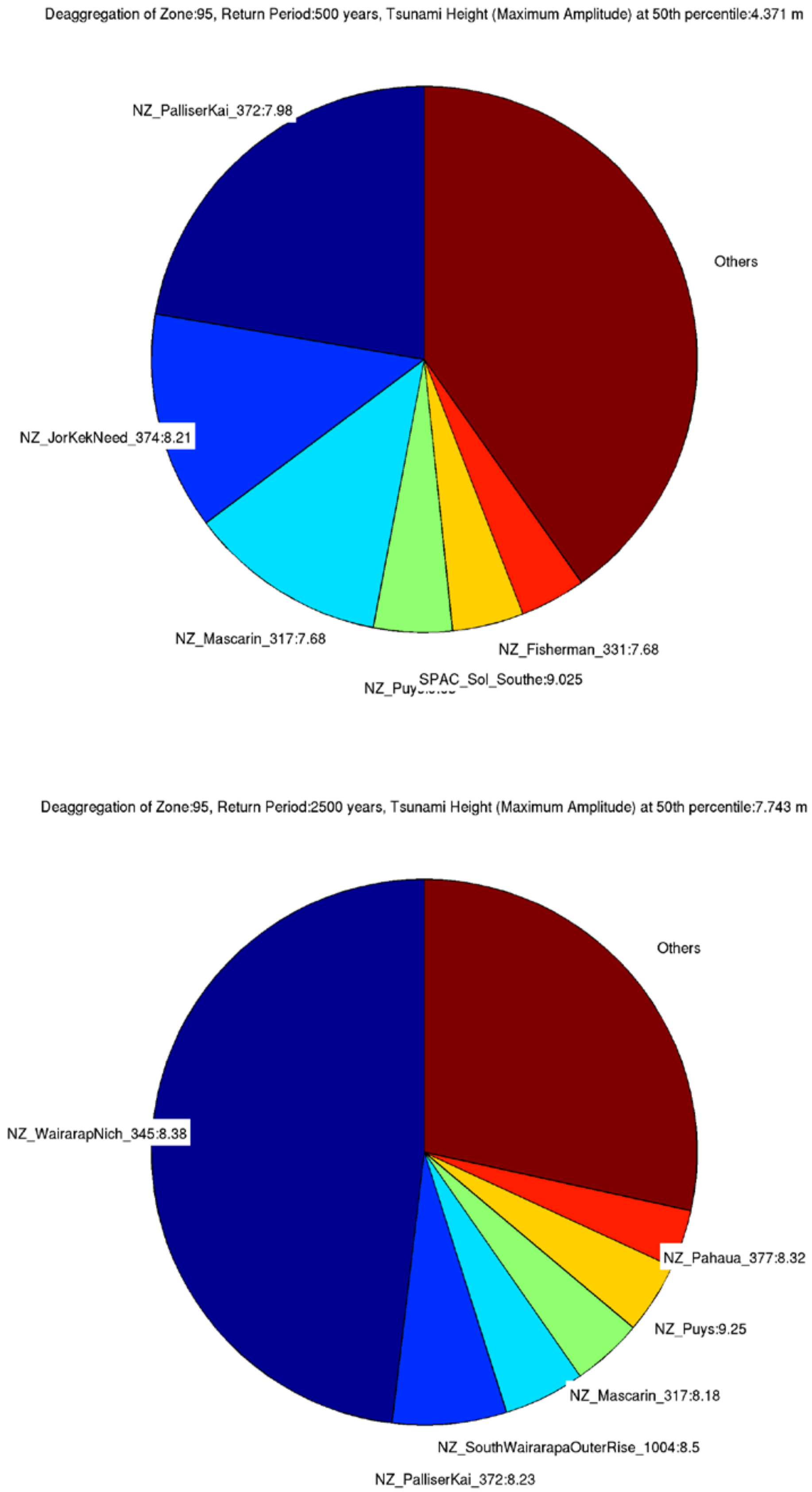

Figure 6.18 Deaggregation of tsunami sources for Kapiti Coast at 500 yr (top) and 2500 yr (bottom) return periods.

Napier

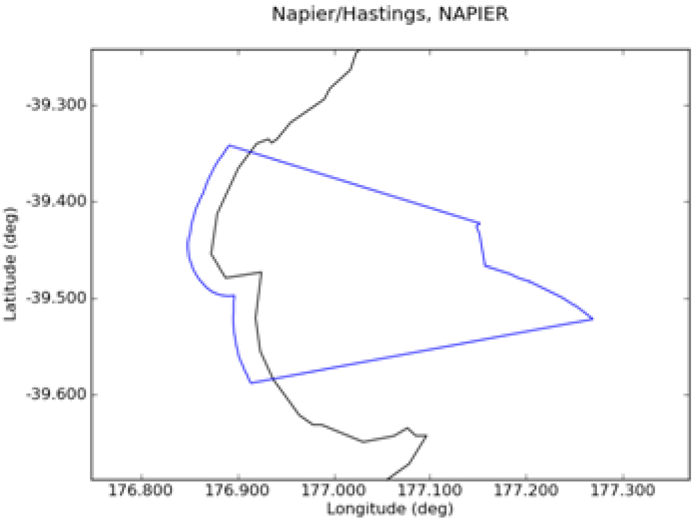

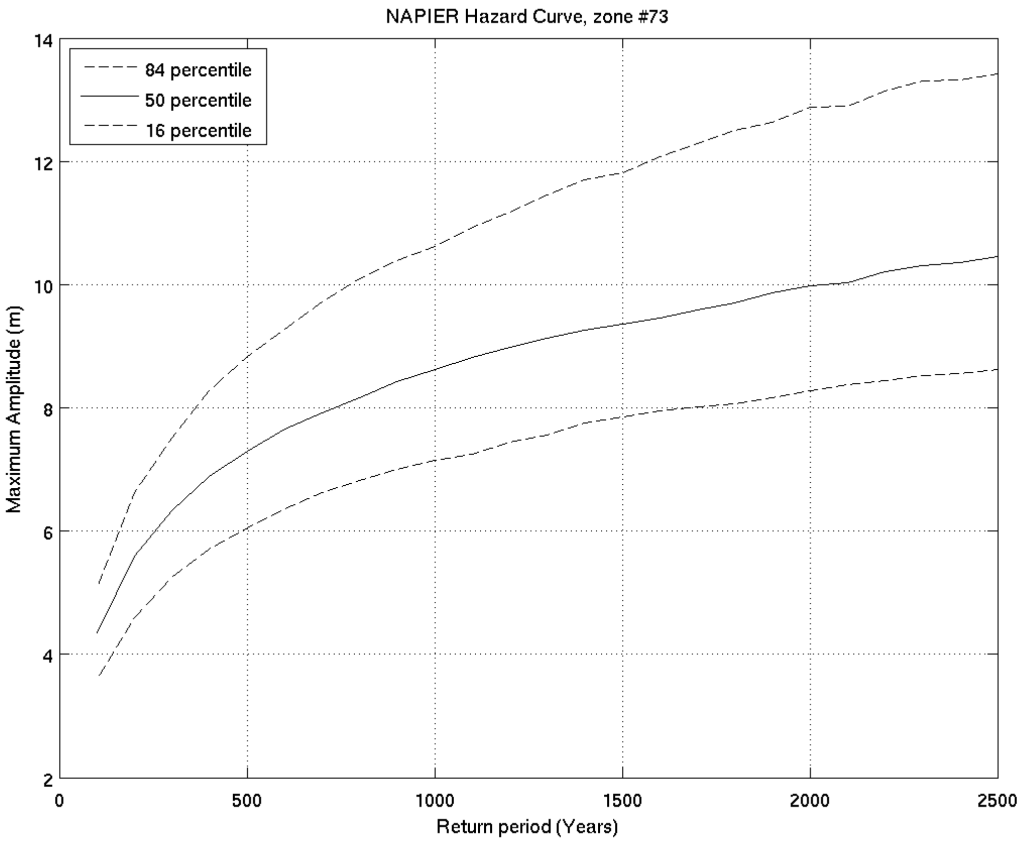

Figure 6.19 Area map and tsunami hazard curve for Napier.

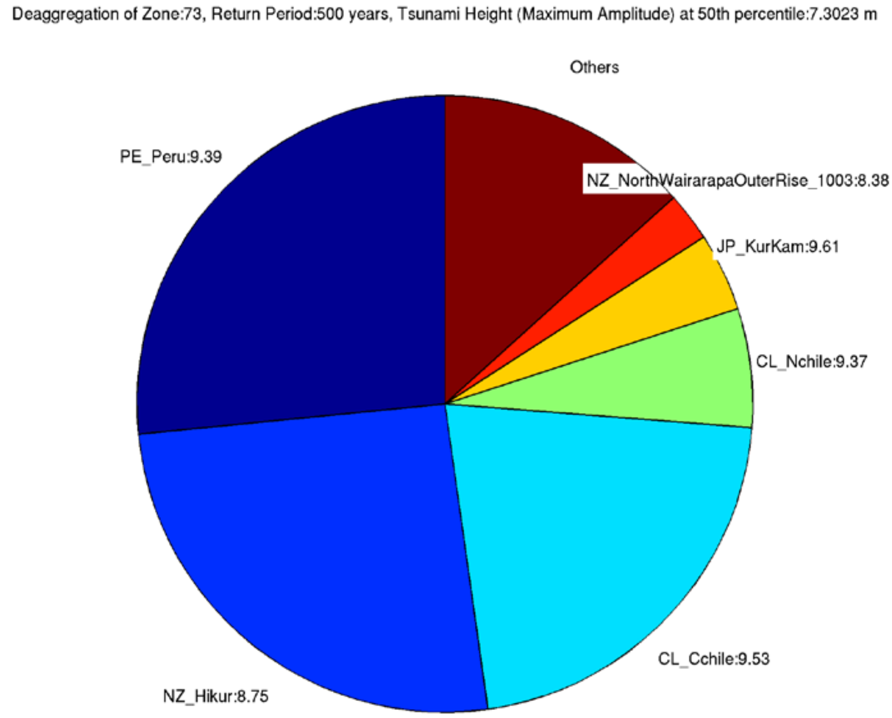

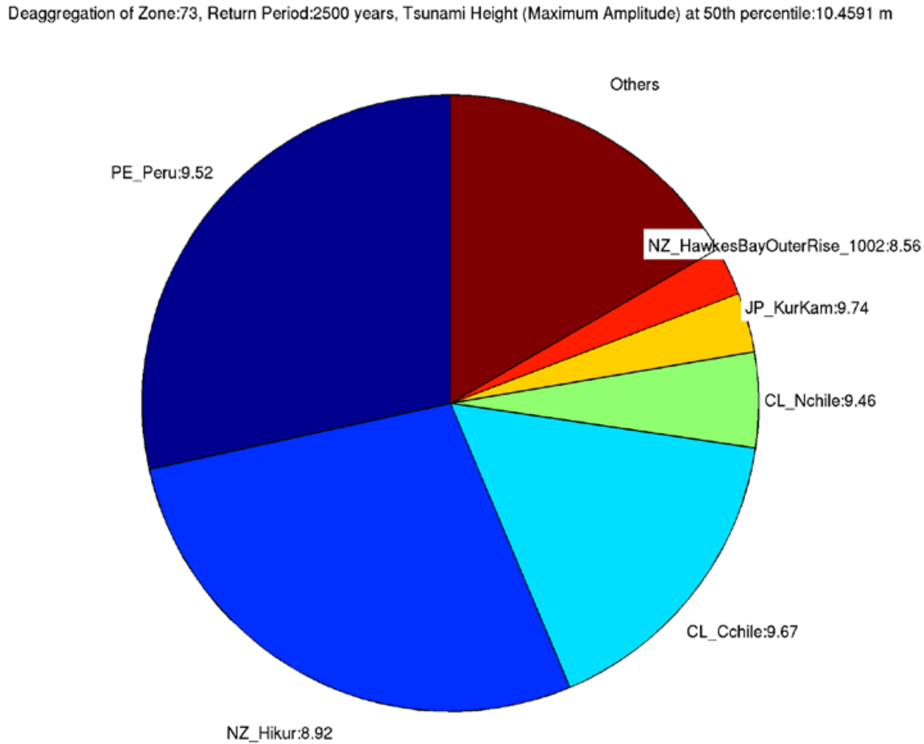

Figure 6.20 Deaggregation of tsunami sources for Napier at 500 yr (top) and 2500 yr (bottom) return periods.

Nelson

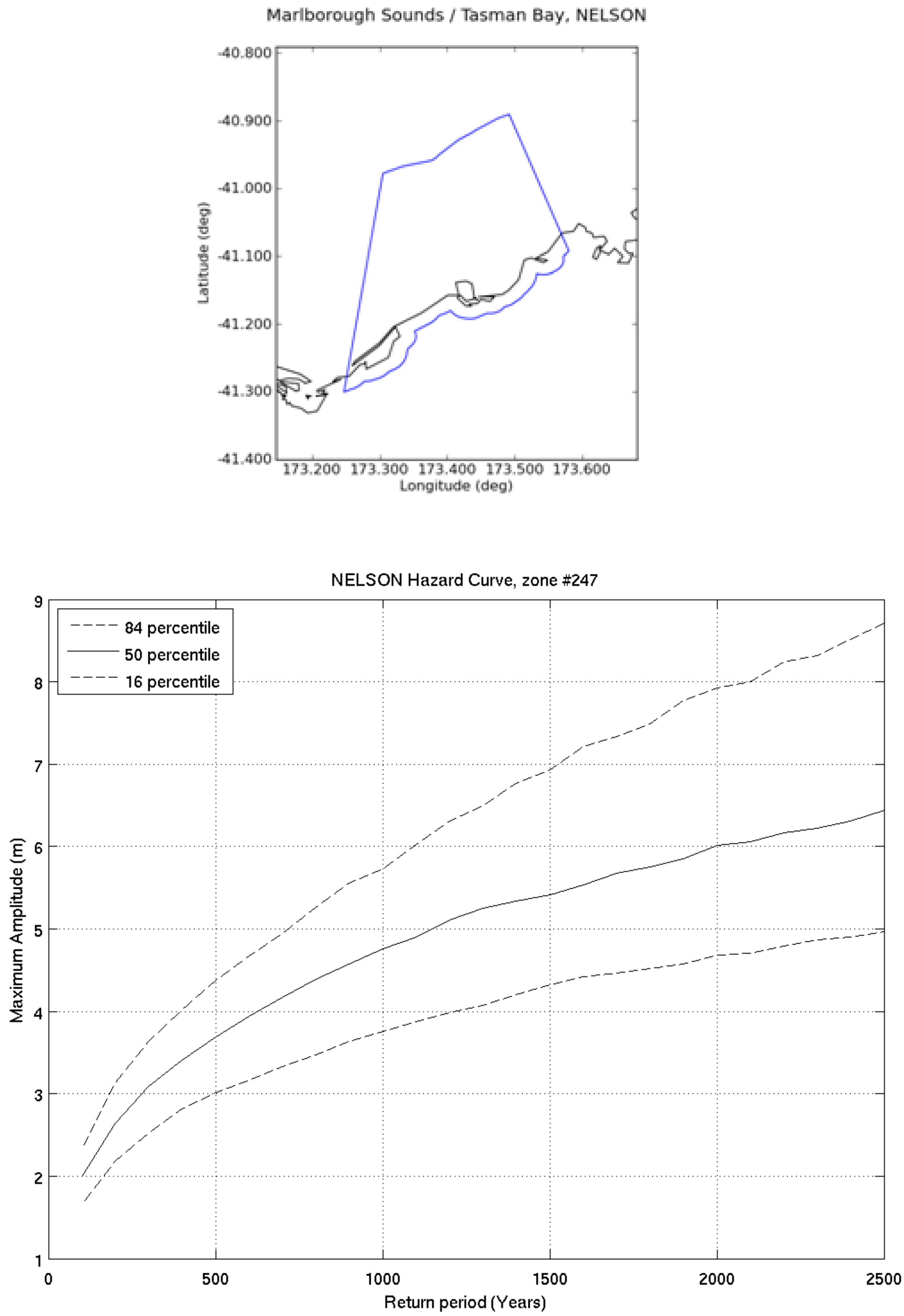

Figure 6.21 Area map and tsunami hazard curve for Nelson.

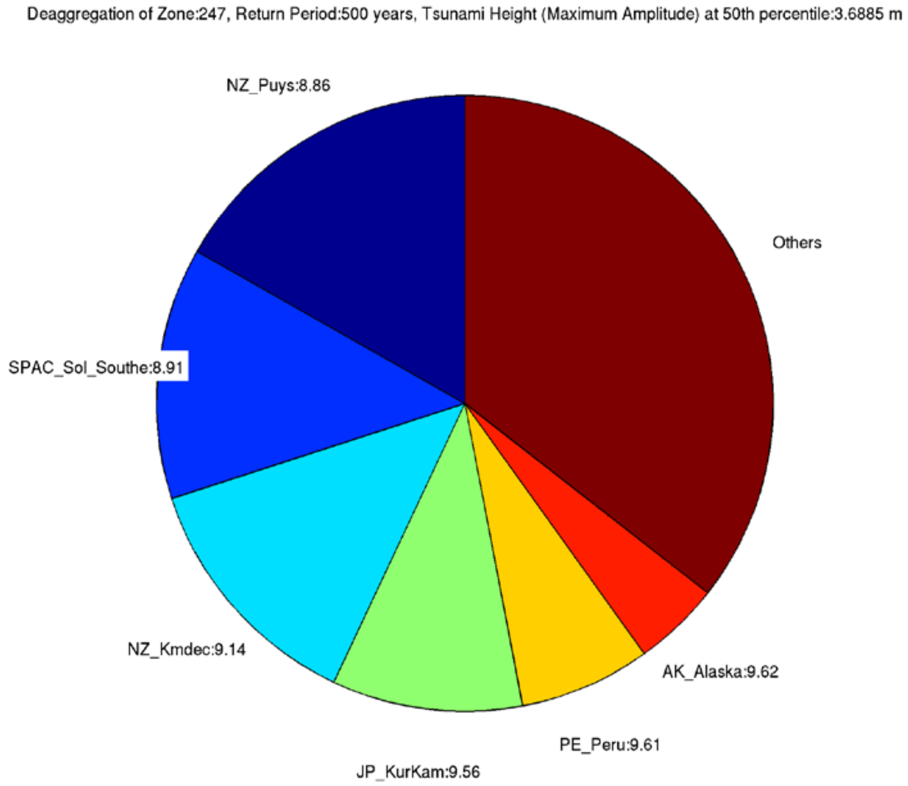

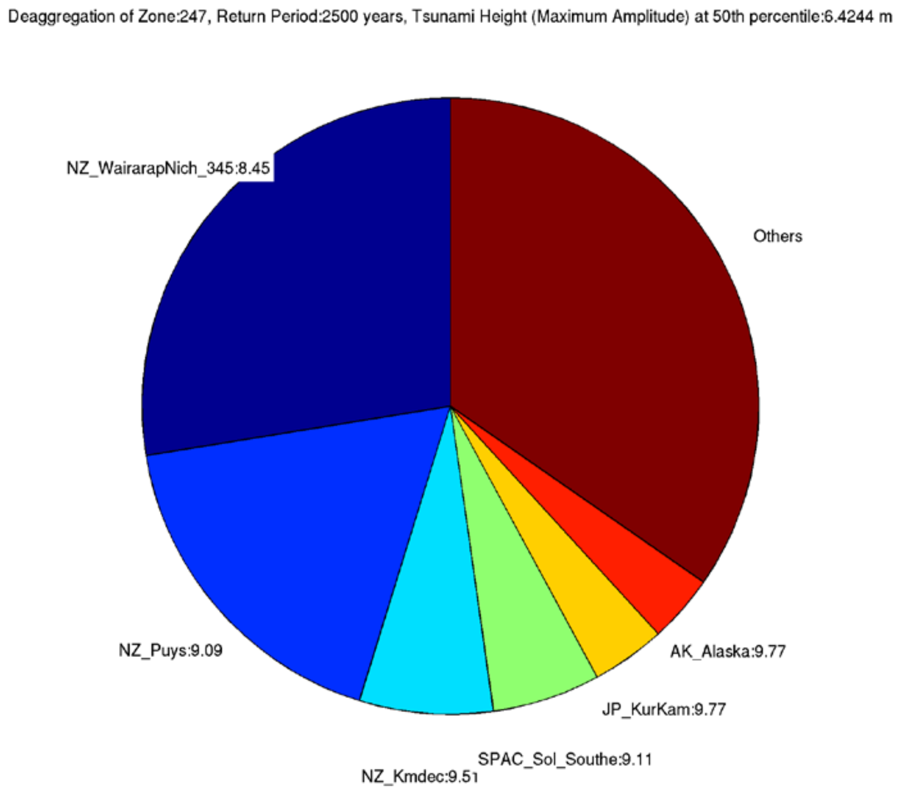

Figure 6.22 Deaggregation of tsunami sources for Nelson at 500 yr (top) and 2500 yr (bottom) return periods.

New Plymouth

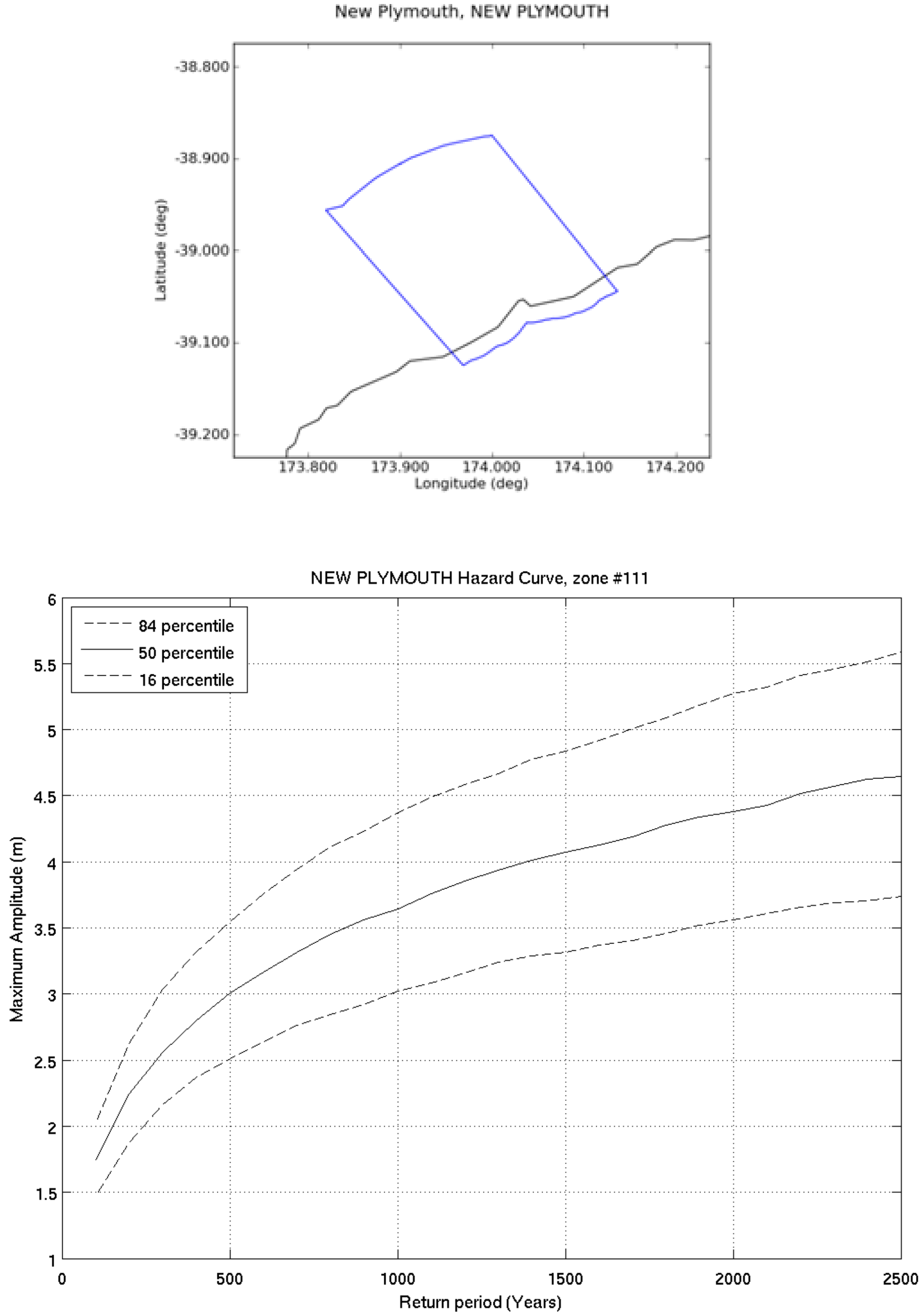

Figure 6.23 Area map and tsunami hazard curve for New Plymouth.

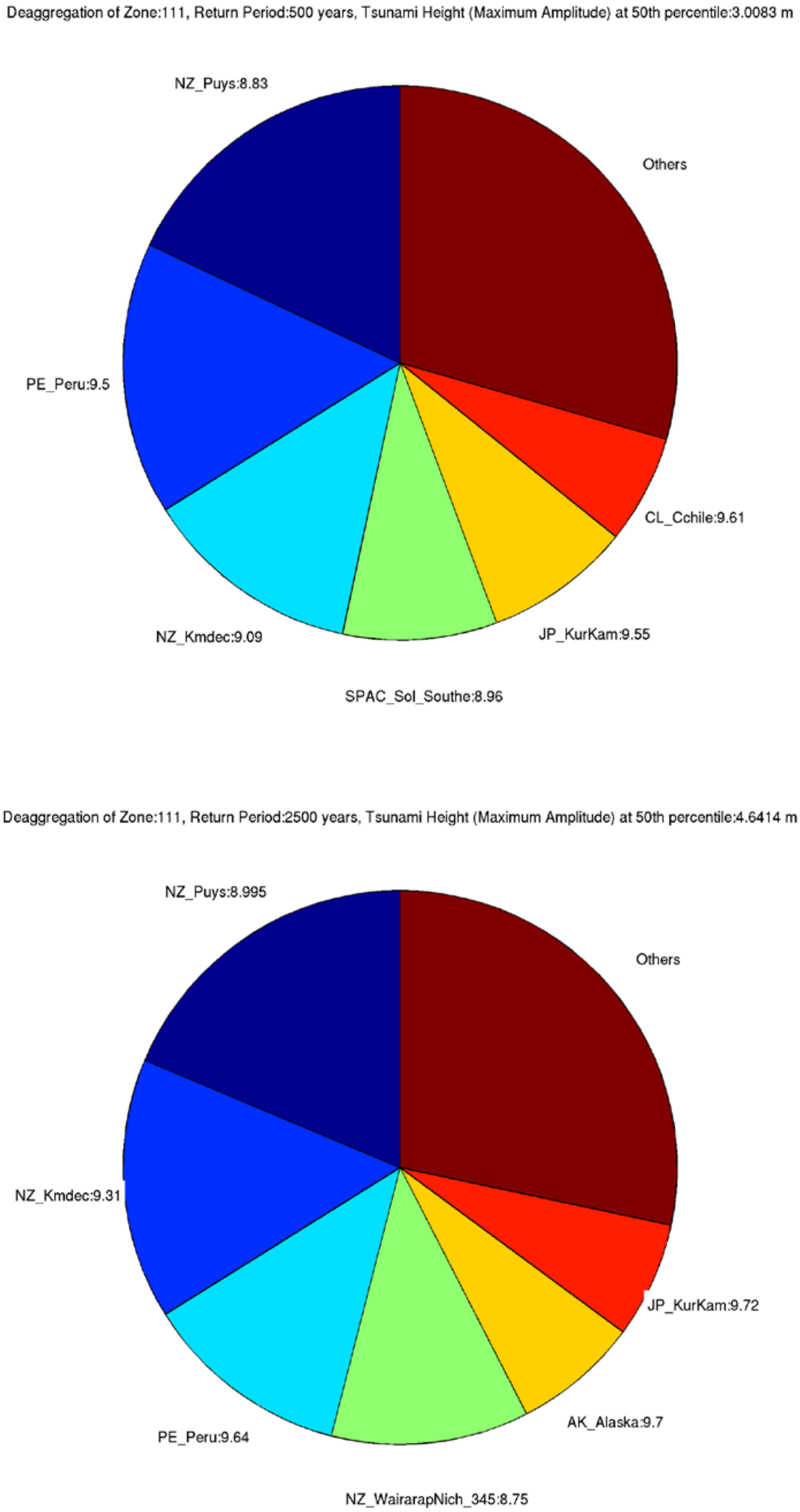

Figure 6.24 Deaggregation of tsunami sources for New Plymouth at 500 yr (top) and 2500 yr (bottom) return periods.

Porirua

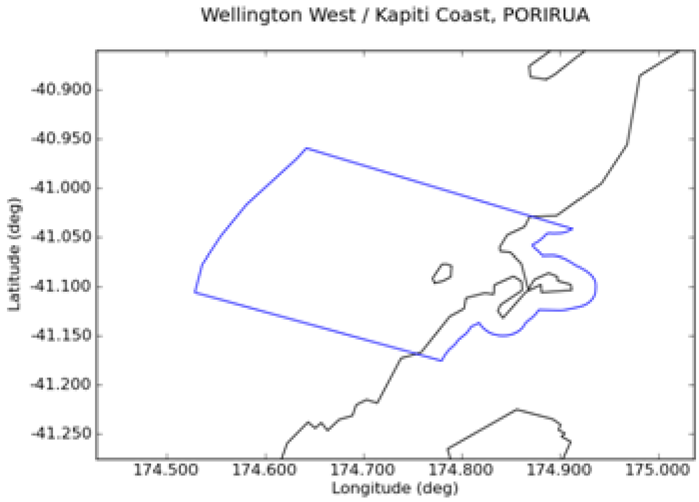

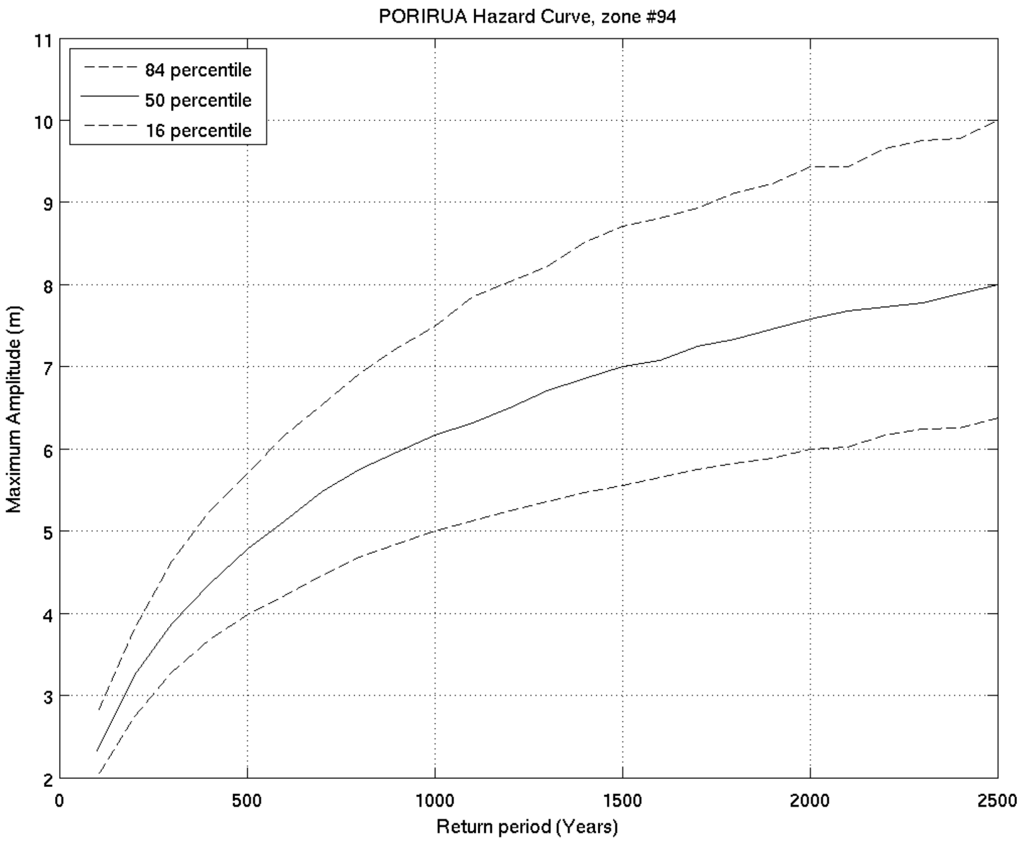

Figure 6.25 Area map and tsunami hazard curve for Porirua.

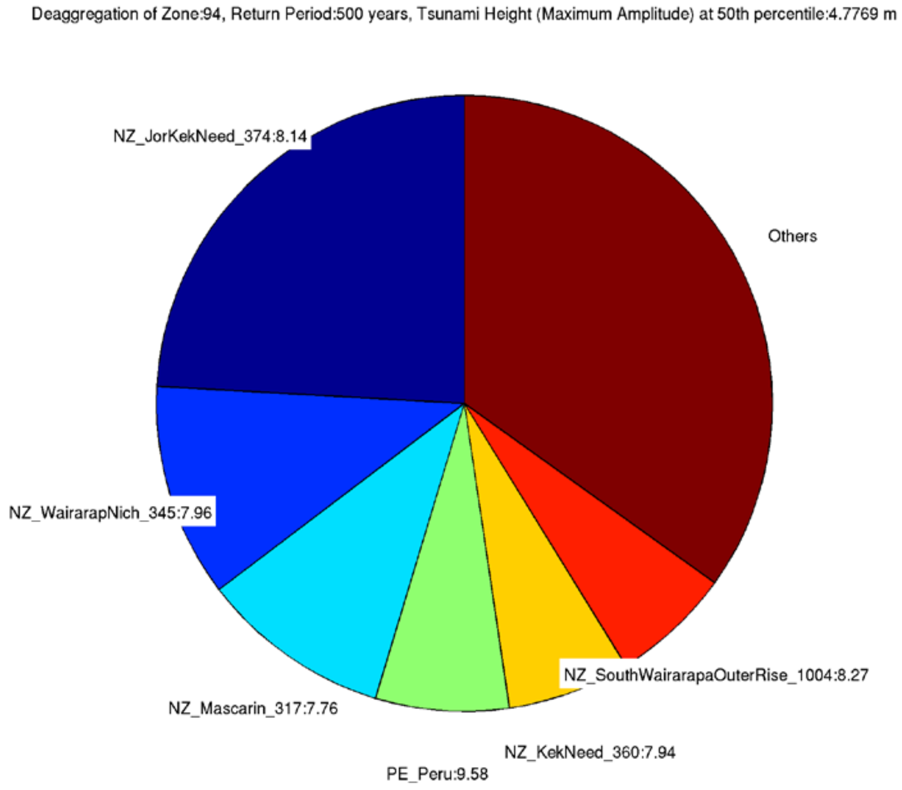

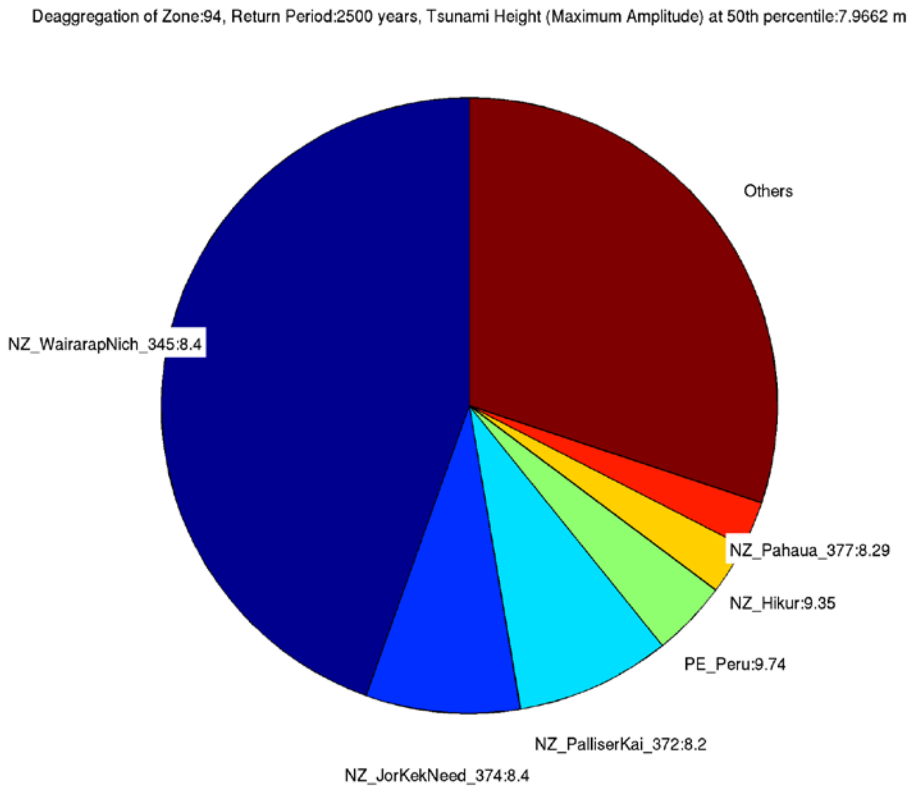

Figure 6.26 Deaggregation of tsunami sources for Porirua at 500 yr (top) and 2500 yr (bottom) return periods.

Tauranga

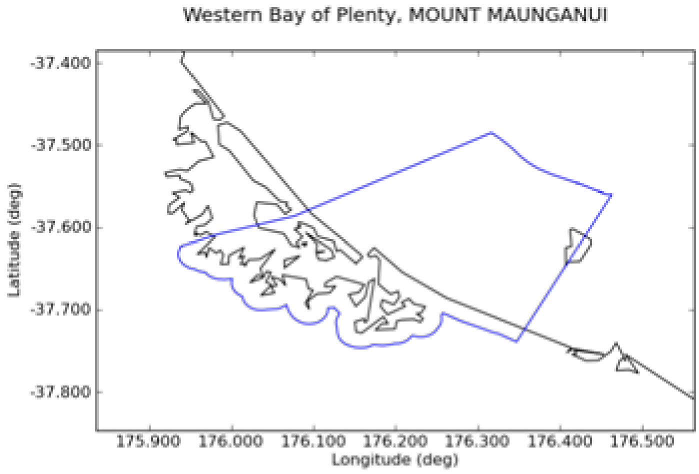

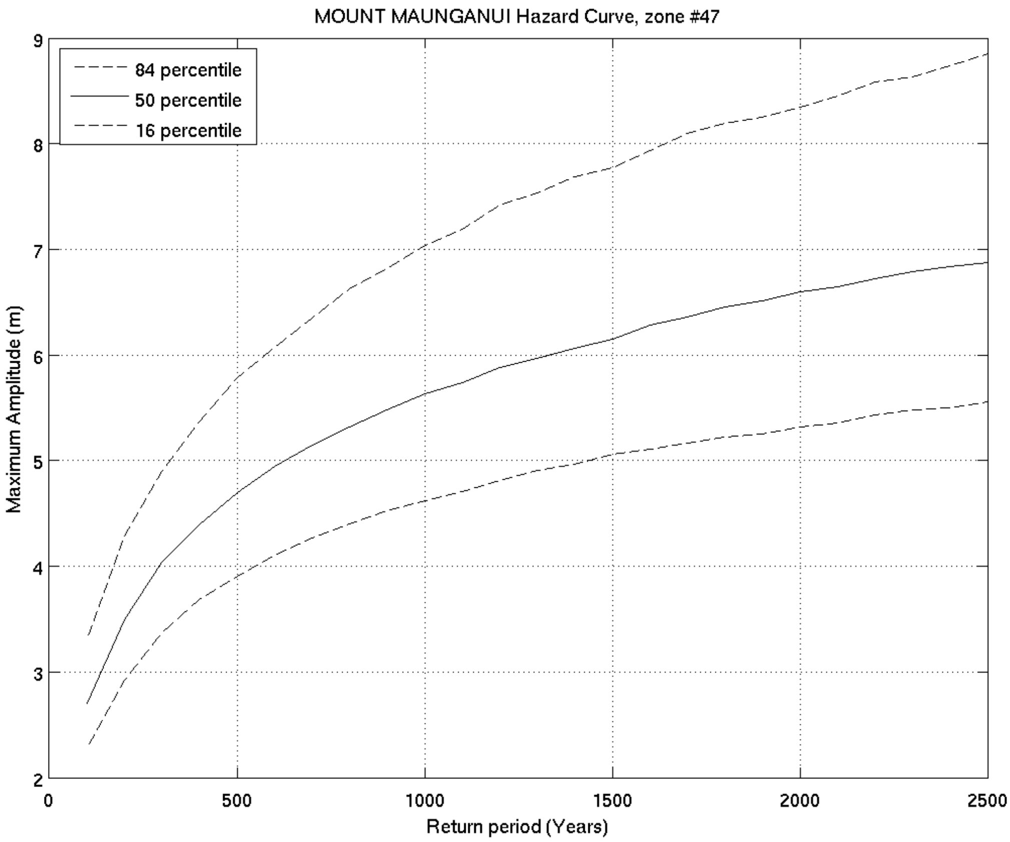

Figure 6.27 Area map and tsunami hazard curve for Tauranga.

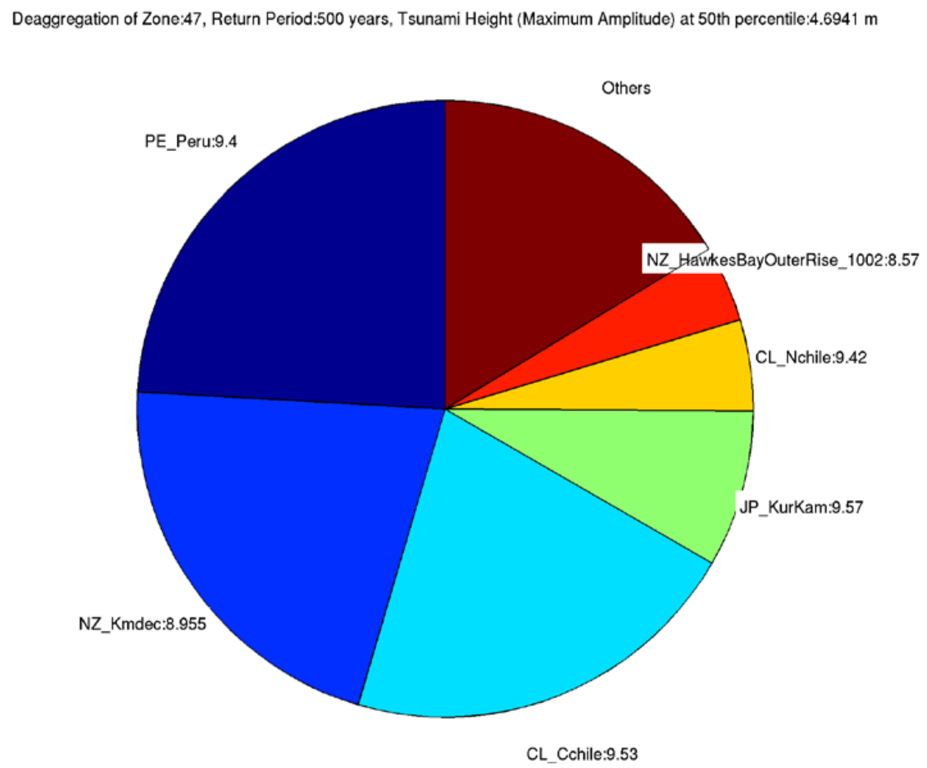

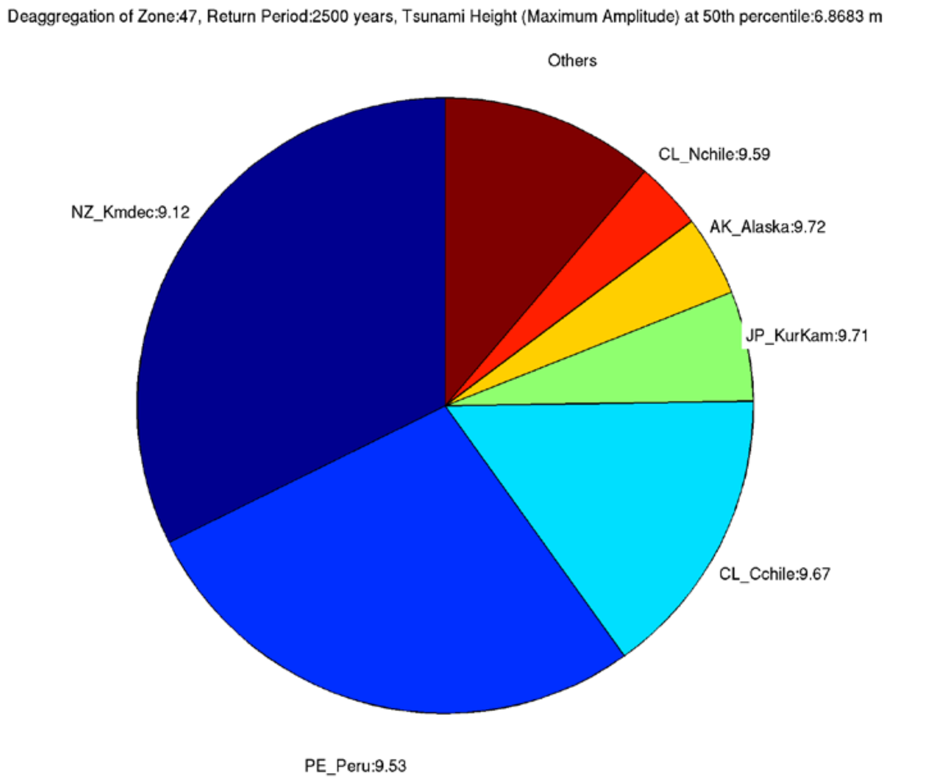

Figure 6.28 Deaggregation of tsunami sources for Tauranga at 500 yr (top) and 2500 yr (bottom) return periods.

Timaru

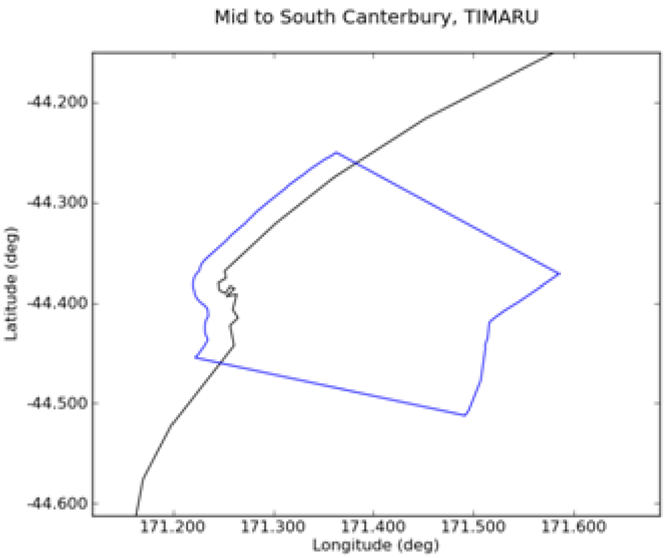

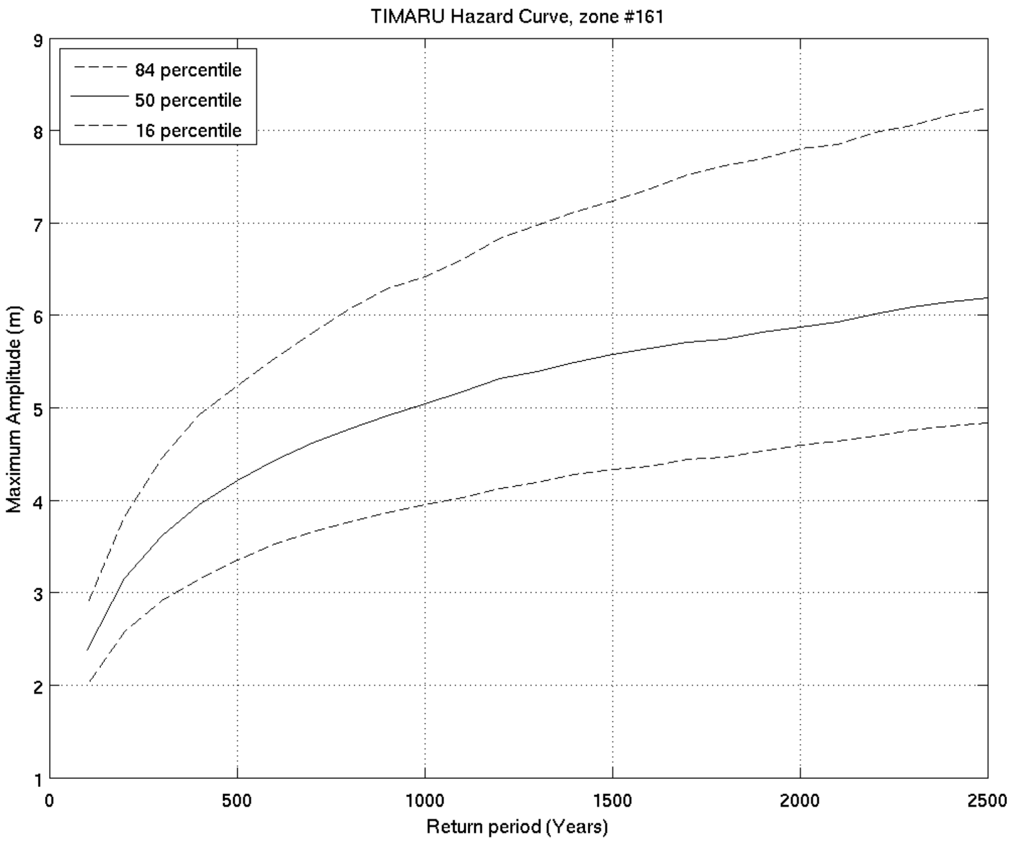

Figure 6.29 Area map and tsunami hazard curve for Timaru.

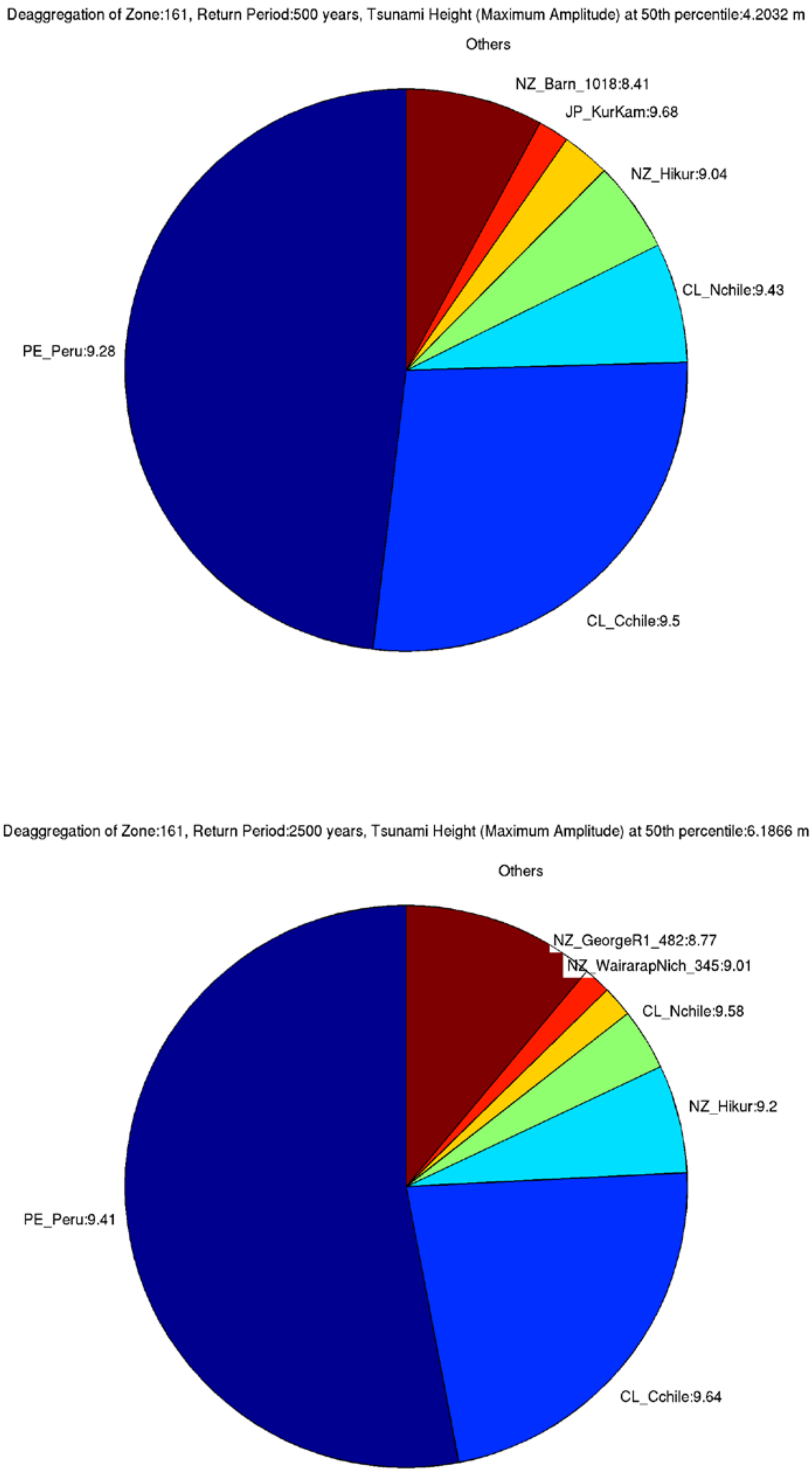

Figure 6.30 Deaggregation of tsunami sources for Timaru at 500 yr (top) and 2500 yr (bottom) return periods.

Wellington

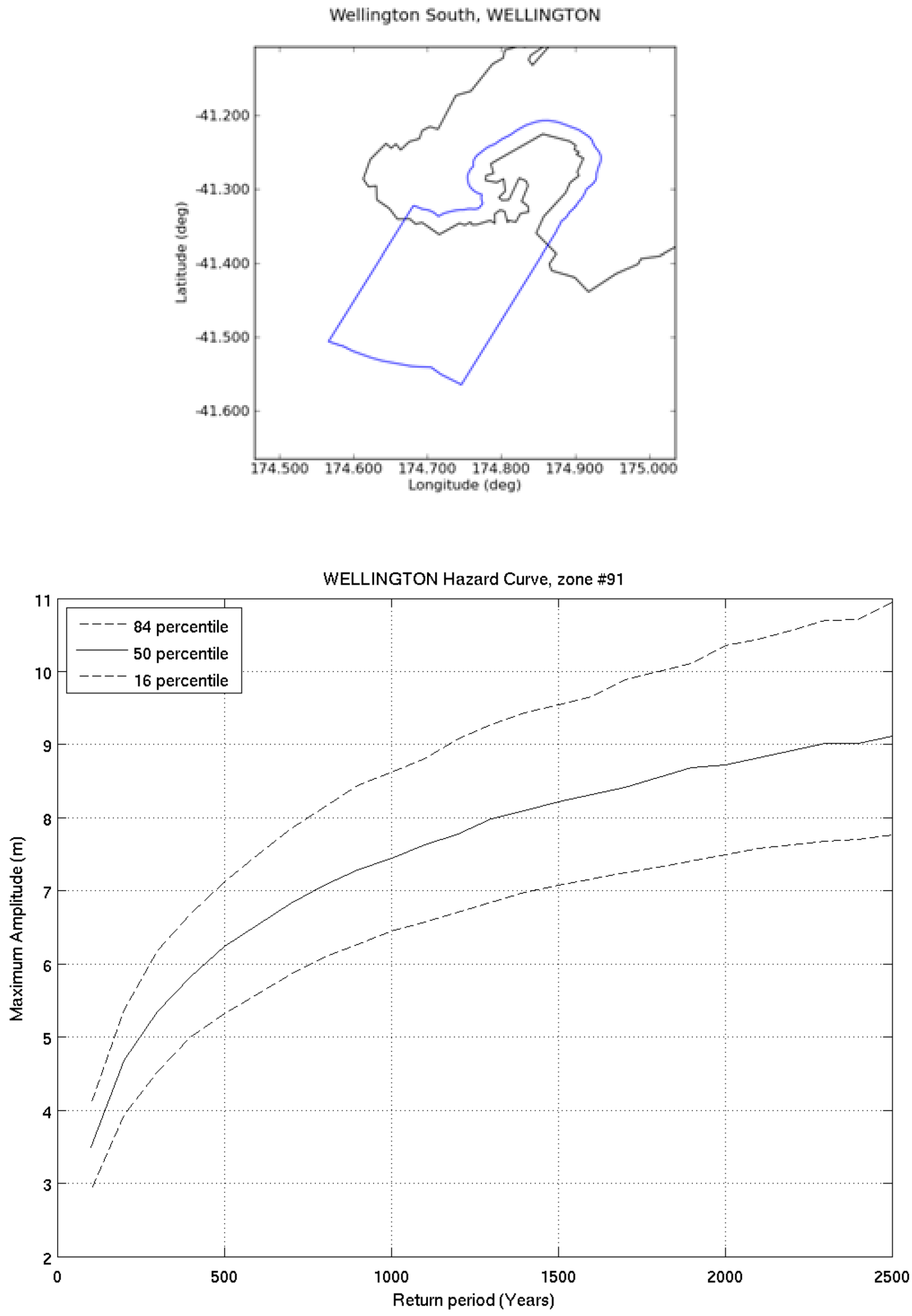

Figure 6.31 Area map and tsunami hazard curve for Wellington.

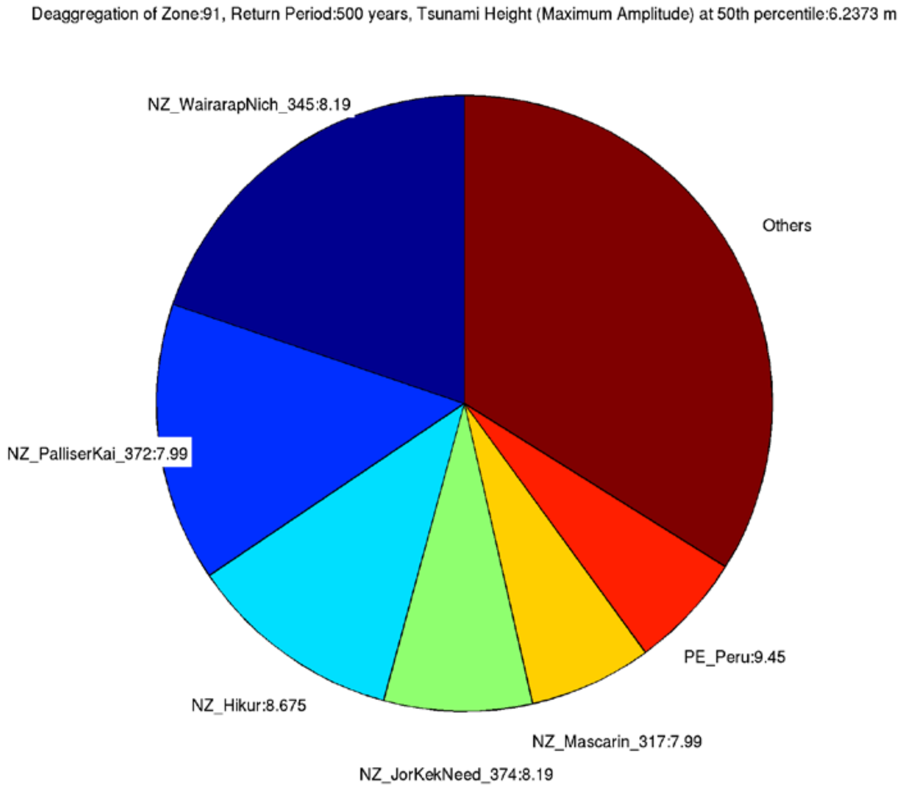

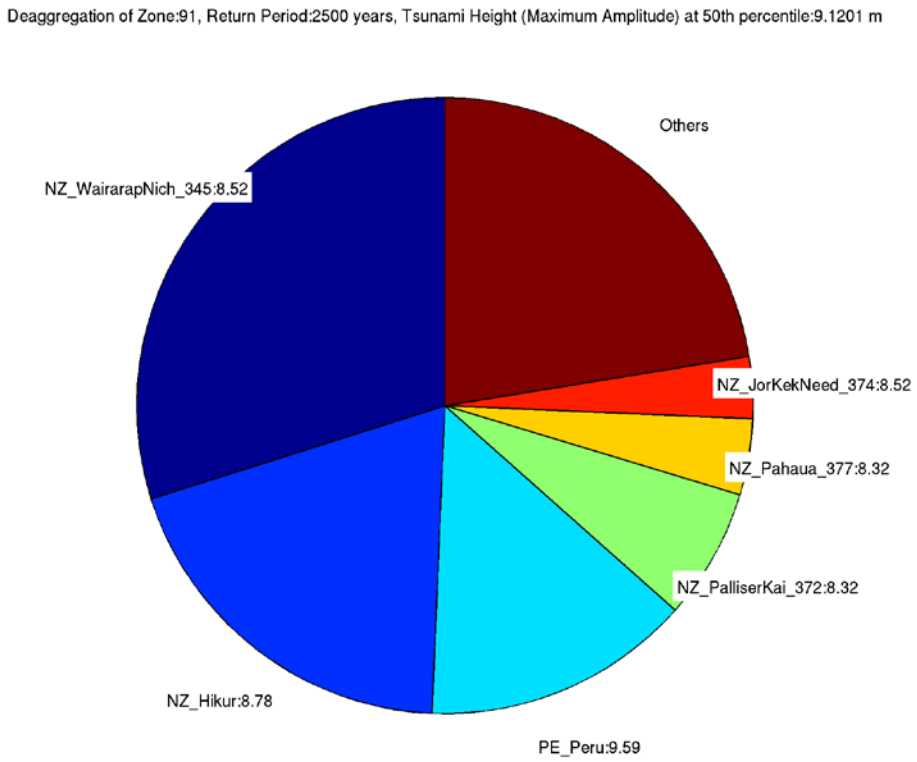

Figure 6.32 Deaggregation of tsunami sources for Wellington at 500 yr (top) and 2500 yr (bottom) return periods.

Whakatane

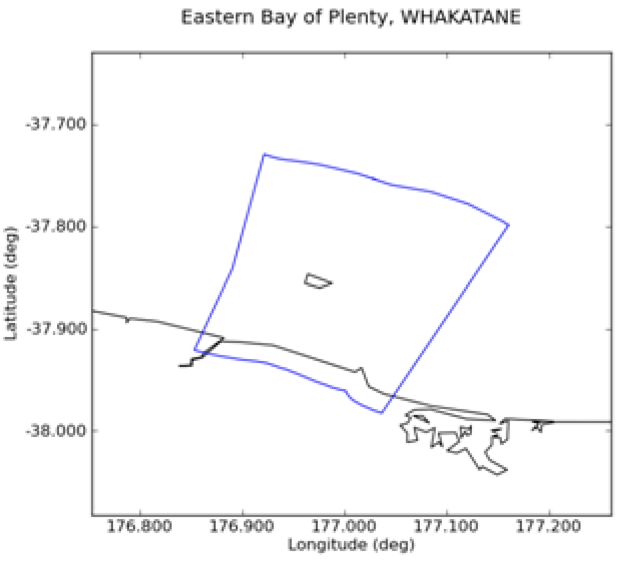

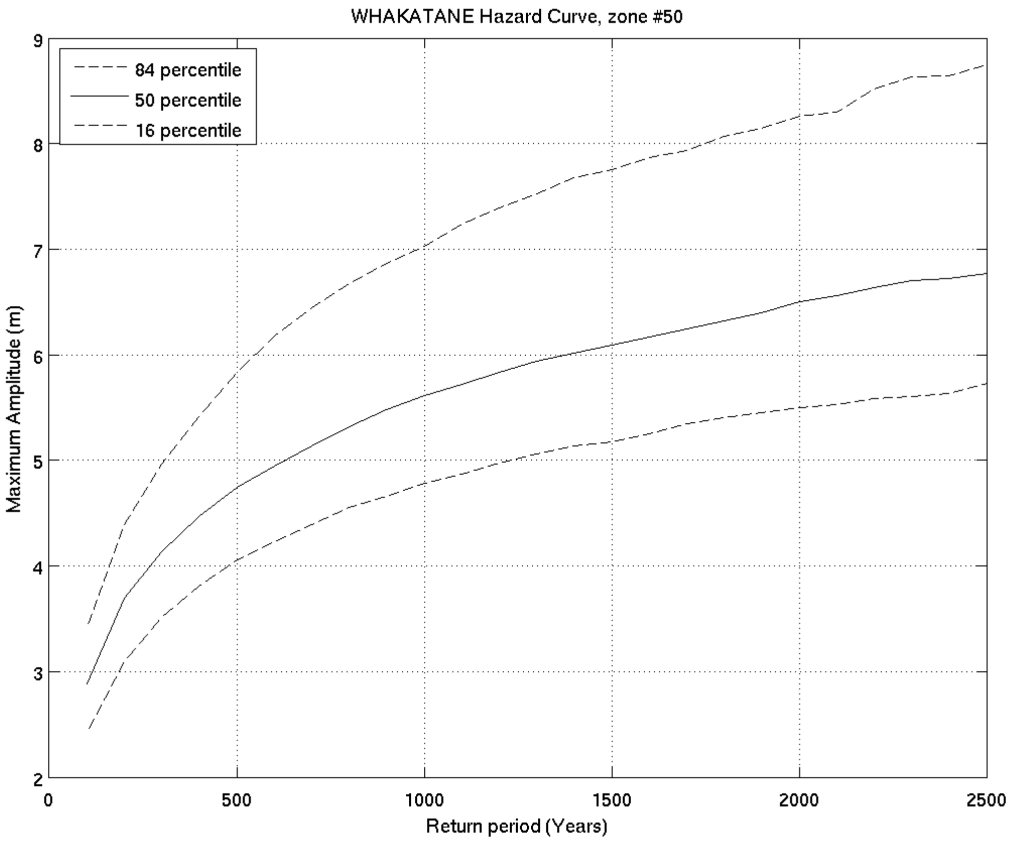

Figure 6.33 Area map and tsunami hazard curve for Whakatane.

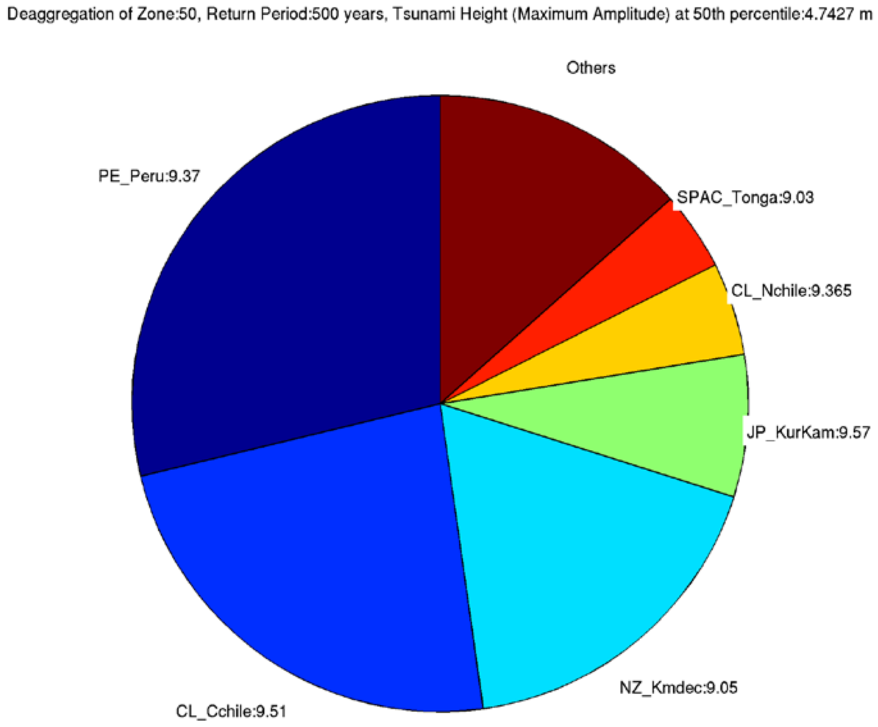

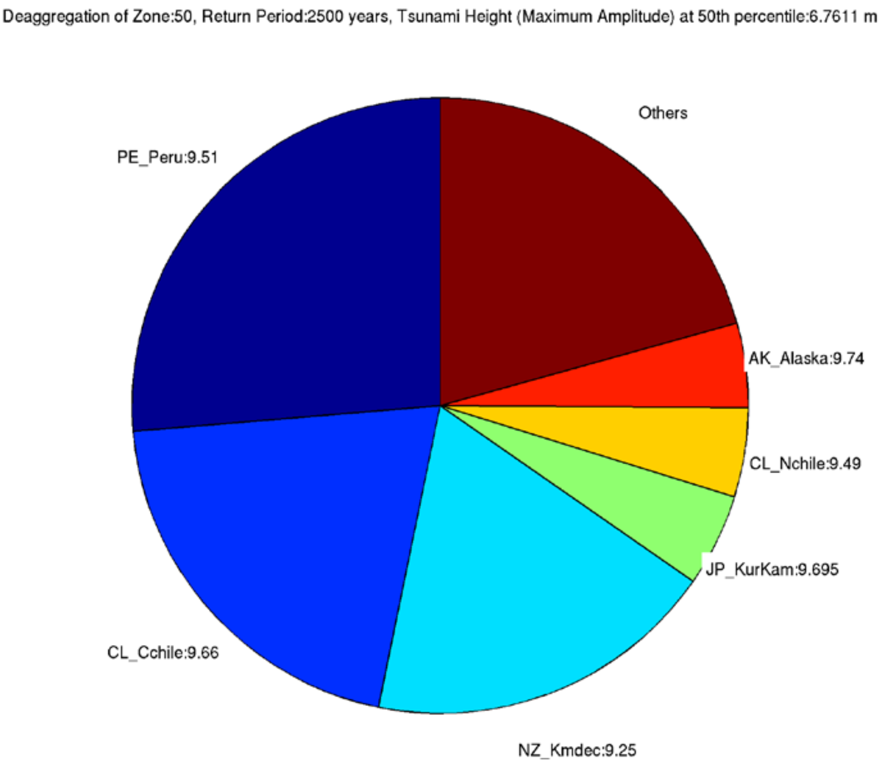

Figure 6.34 Deaggregation of tsunami sources for Whakatane at 500 yr (top) and 2500 yr (bottom) return periods.

Whangarei

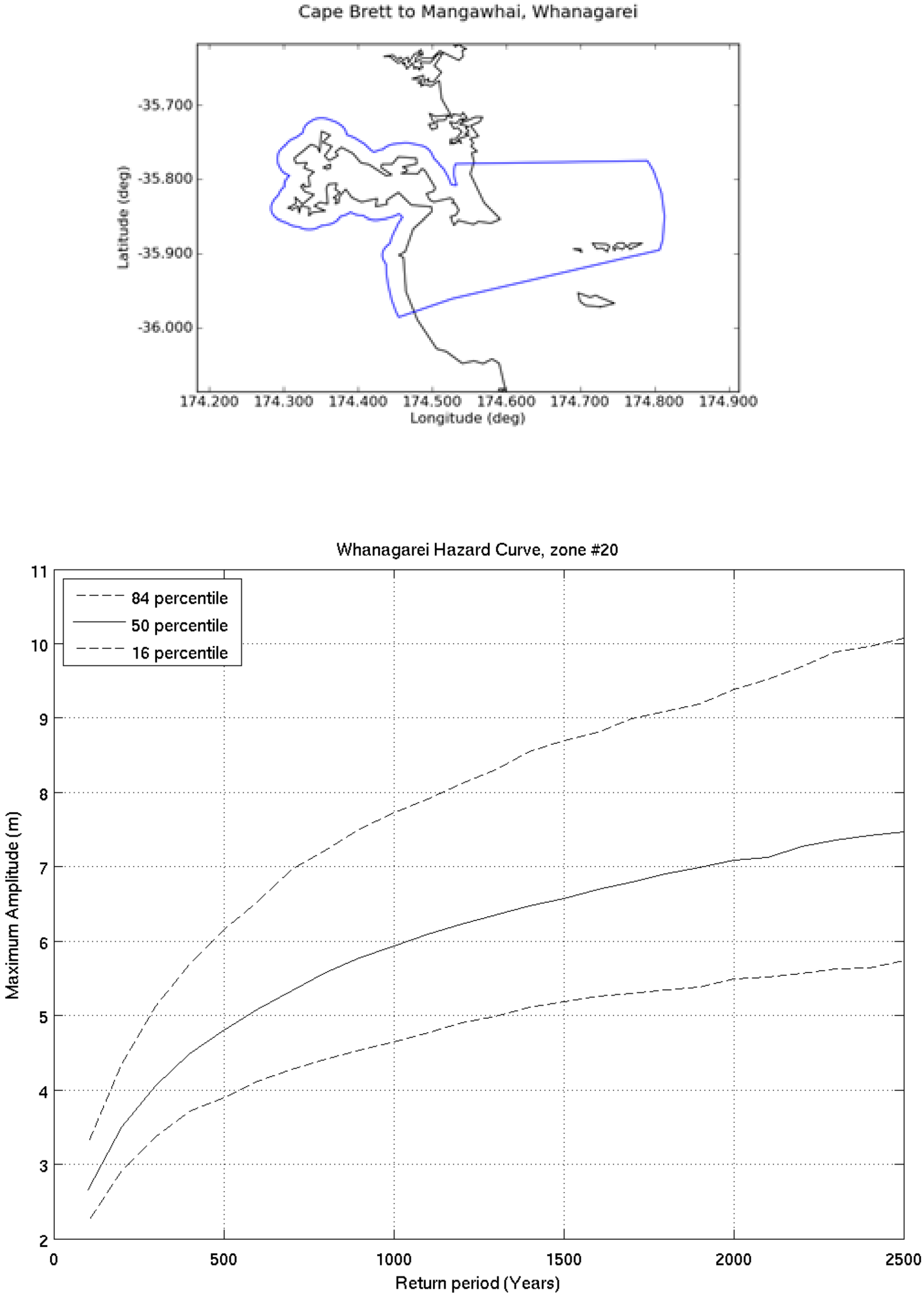

Figure 6.35 Area map and tsunami hazard curve for Whangarei.

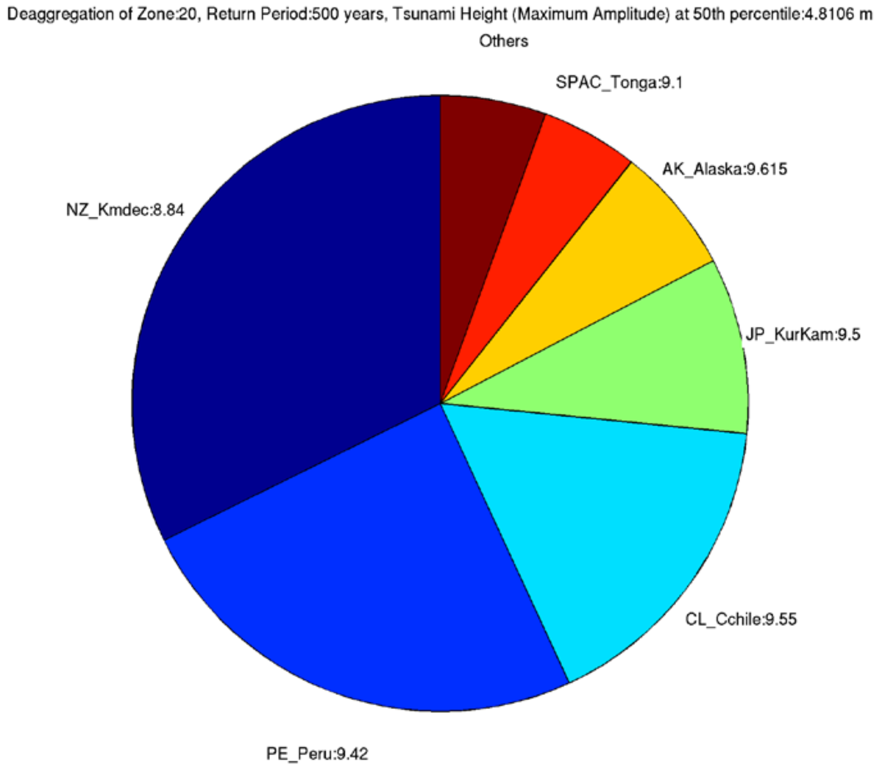

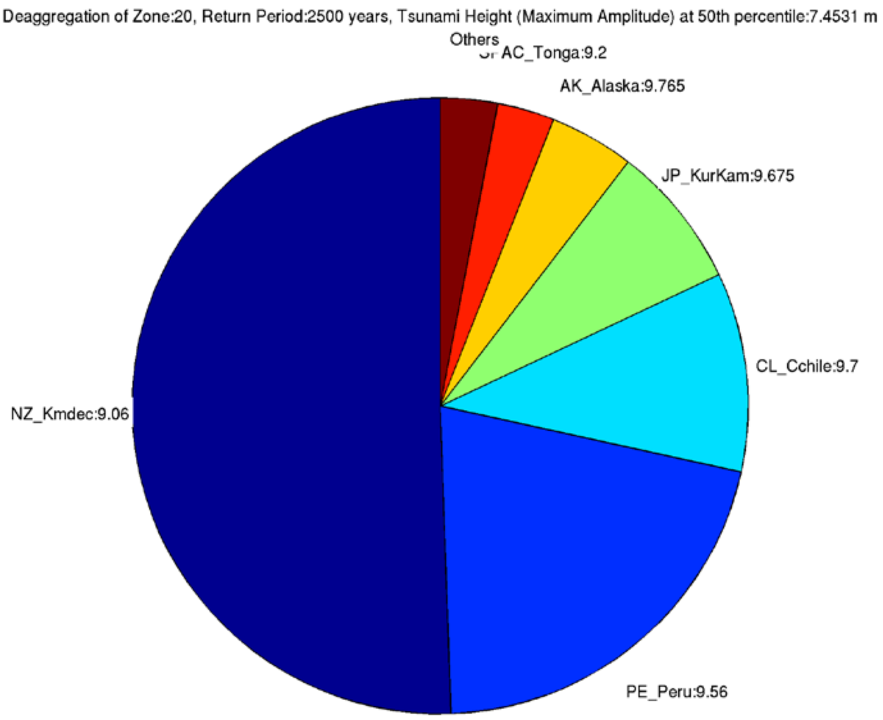

Figure 6.36 Deaggregation of tsunami sources for Whangarei at 500 yr (top) and 2500 yr (bottom) return periods.

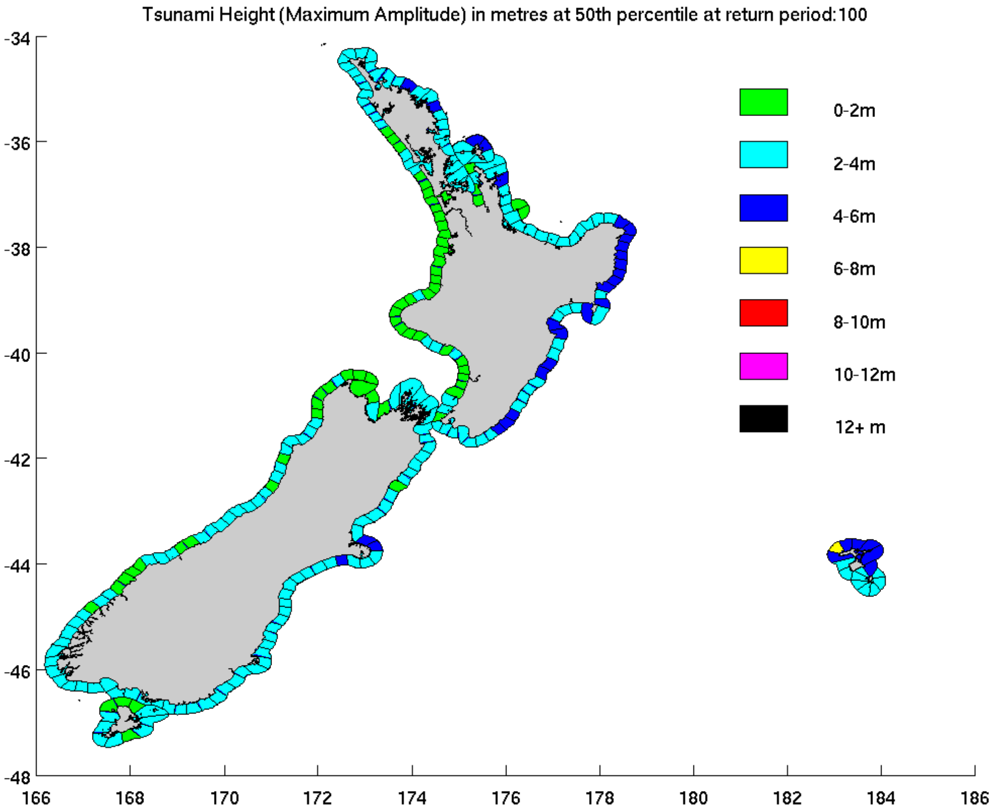

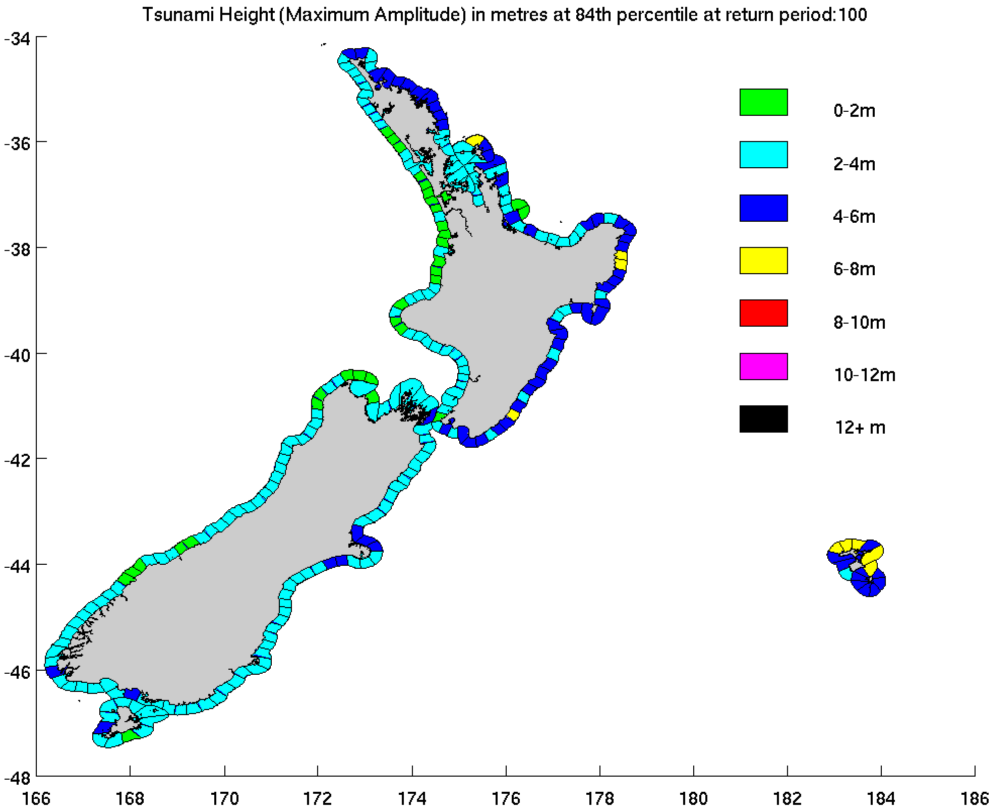

Figure 6.37 Expected maximum tsunami height in metres at 100 year return period, shown at median (50th percentile) and 84th percentile of epistemic uncertainty. See comment on the Wairarapa coast in Section 6.10.

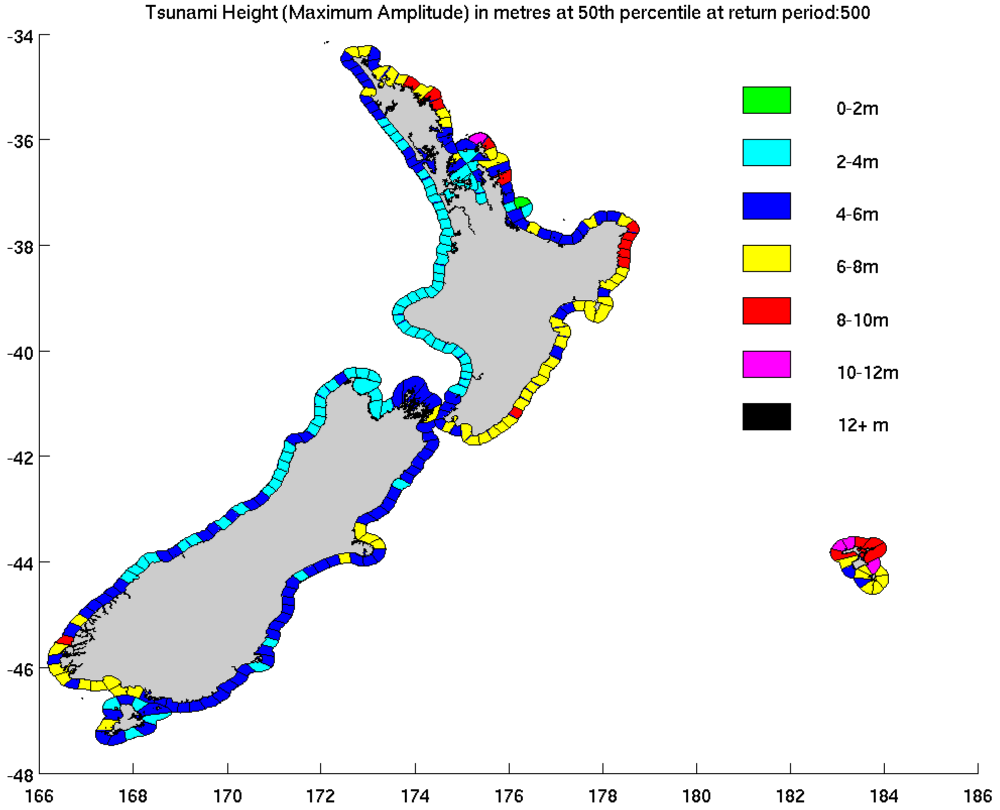

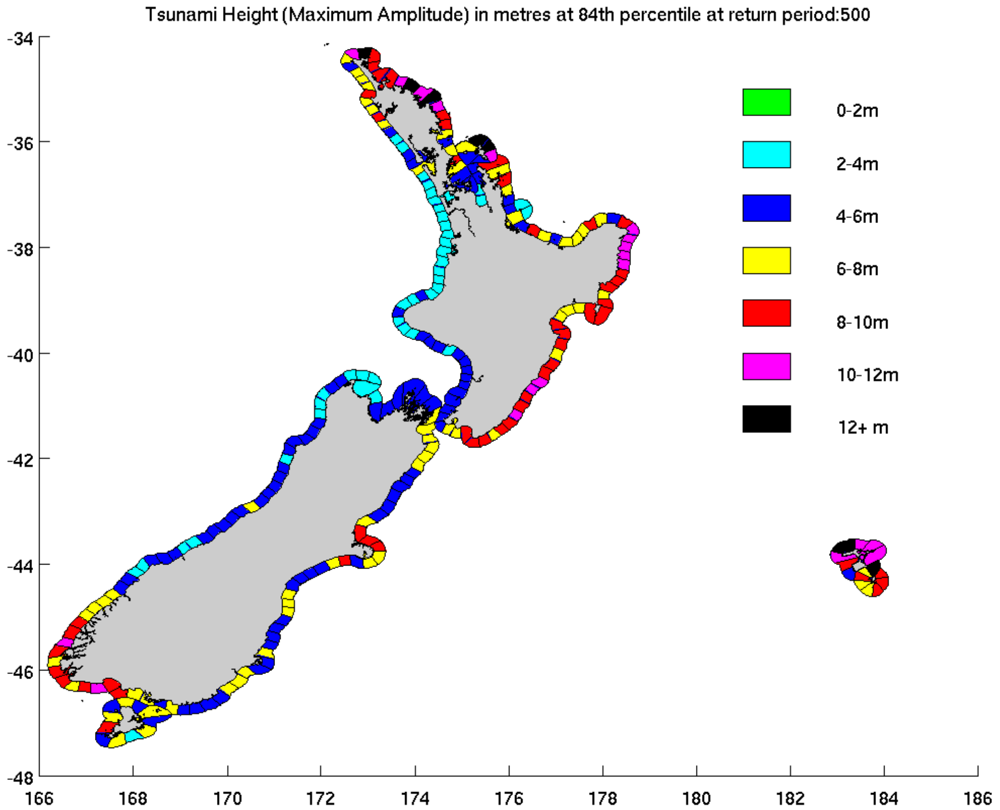

Figure 6.38 Expected maximum tsunami height in metres at 500 year return period, shown at median (50th percentile) and 84th percentile of epistemic uncertainty.

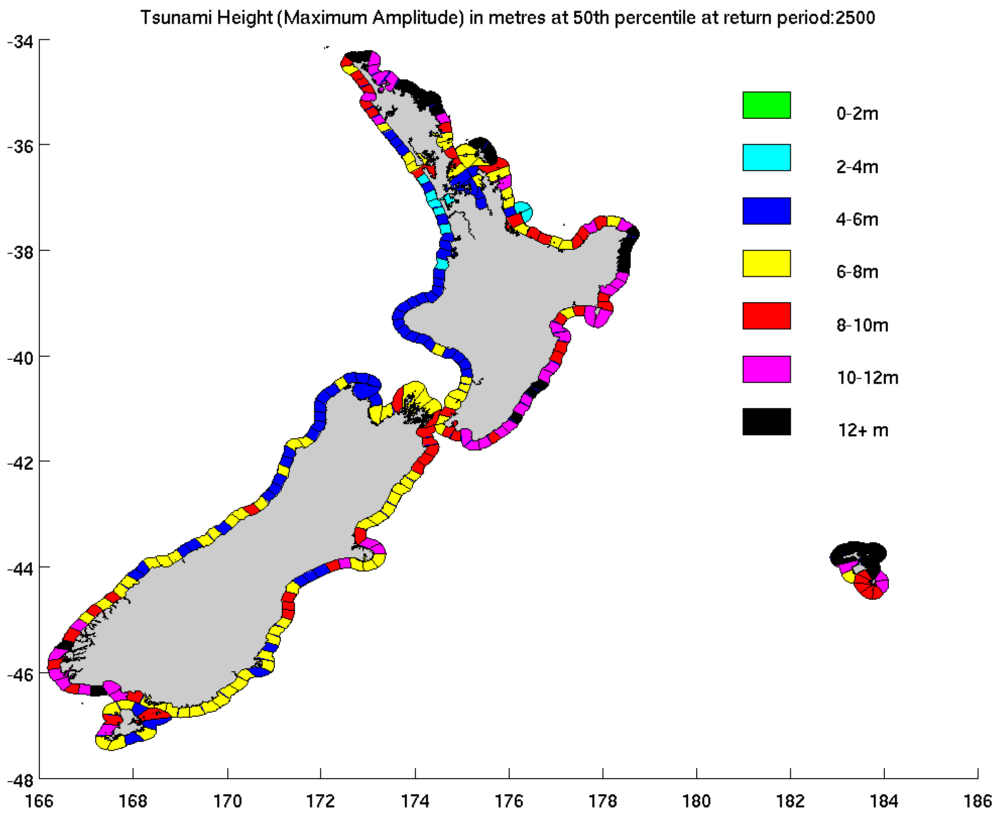

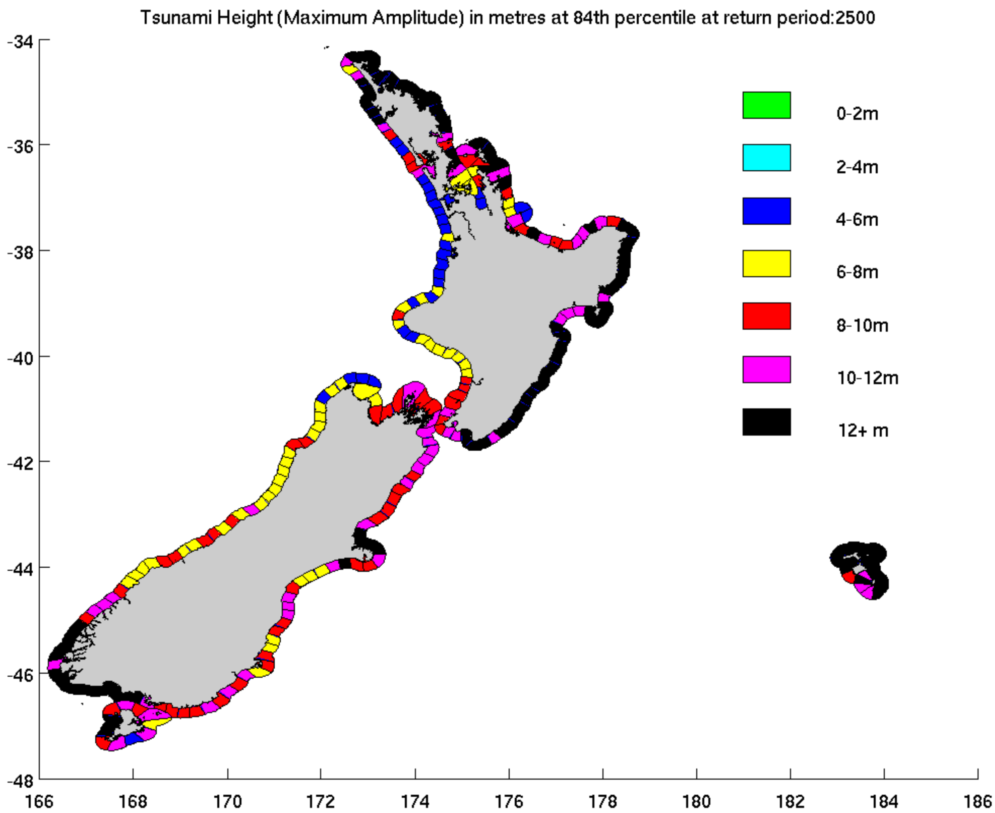

Figure 6.39 Expected maximum tsunami height in metres at 2500 year return period, shown at median (50th percentile) and 84th percentile of epistemic uncertainty.

6.10 COMMENTS AND DISCUSSION OF RESULTS

- The nationwide distribution of tsunami hazard is generally consistent with expectations, showing a higher hazard in those areas of the coast directly exposed to local subduction zones and an overall trend for the east coast to be exposed to a higher tsunami hazard than the west coast.
- For most parts of New Zealand, the distribution of tsunami hazard is quite similar to that in the 2005 report to the Ministry of Civil Defence & Emergency Management, *Review of Tsunami Hazard and Risk in New Zealand* (IGNS client report 2005/104). However the coasts that are most exposed to local subduction zones, notably the east-facing coasts of the North Island and the southwest corner of the South Island, are now typically assessed as having a higher tsunami hazard than was estimated in 2005.
- The probabilistic model does not currently take into account variations in geophysical properties within subduction zones. This is an important issue for the Hikurangi Trench, where the northern portions experience weaker coupling and faster convergence than the southern portions.
- The probabilistic model currently does not treat ‘tsunami earthquakes’ (see Section 5.3.1.2) on the shallowest parts of subduction interfaces as being distinct from other subduction interface earthquakes.
- The estimated tsunami hazard around the Kapiti/Manawatu coast and the north coast of the South Island may be overstated because the method used to model tsunami caused by crustal faults in the Wairarapa/Marlborough area does not take into account the dampening effect due to the constriction in Cook Strait (see Appendix 7.4, under ‘Estimation of tsunami heights – Local crustal and outer rise faults’).
- The division of the Pacific Rim into distinct subduction zones (Appendix 3) is in some cases based on distinct geophysical changes, but in some locations the boundaries between subduction zones are more artificial. In some regions subduction earthquakes may have ruptures that span more than one zone, a situation not represented in the current model.

The probabilistic tsunami hazard model represents the best endeavours of the report authors at the time it was created. Scientific understanding of input parameters will continue to evolve, and improved methods for calculating the hazard will be developed. The programs used to perform the calculations are complicated, and programming errors may be found and corrected. Hence the results in this report represent only a snapshot of the estimated tsunami hazard, as determined at the time of its construction.

6.11 FUTURE WORK

The method used for estimating tsunami heights for the local non-subduction zone faults is of low accuracy (high uncertainty), and in the long term it would be better to replace this with scaled-numerical modelling results. As the development of such models is difficult, it is useful to prioritise, so that the most important sources are developed first. Ranking our sources by the annualised moment release, i.e., the average seismic moment release per year, gives the following priority list:

Table 6.2 New Zealand local faults ranked by rate of moment release. See Appendix 4 for fault details. Location of faults can be identified using the NZSHM code and figures in Stirling et al. (2012).

Rank	Name and NZSHM code	M_W	Recurrence Interval (yrs)	Seismic moment/year
1	WairarapNich_345	8.2	1199	2.10E+18
2	JorKekNeed_374	7.6	389	8.13E+17
3	RaukumaraOuterRise_1001	7.8	1300	4.85E+17
4	HawkesBayOuterRise_1002	7.8	1460	4.32E+17
5	NorthWairarapaOuterRise_1003	7.8	1640	3.85E+17
6	SouthWairarapaOuterRise_1004	7.8	1900	3.32E+17
7	PalliserKai_372	7.6	1114	2.84E+17
8	Swedge5_492	7.7	1695	2.64E+17
9	GeorgeR1_482	8.1	7104	2.50E+17
10	MilfordB1_469	7.6	1416	2.23E+17
11	ArielBank_202	7.4	723	2.19E+17
12	Lachlan3_231	7.5	1068	2.10E+17
13	Cw4Swedge411_497	7.5	1254	1.79E+17
14	CBalleny_536	7.4	932	1.70E+17
15	JorKekCha_373	7.6	2089	1.51E+17
16	Swedge2_499	7.4	1068	1.48E+17
17	Madden_316	7.6	2396	1.32E+17
18	Barn_1018	7.6	2400	1.32E+17
19	Mataikona_335	7.3	853	1.32E+17
20	Pahaua_377	7.9	6779	1.32E+17

Addition of landslide sources to the probabilistic model is a goal which is discussed in Appendix 6.

Improving the source model definitions, and improving and calibrating the numerical tsunami models, is an on-going task. This is particularly important for the Hikurangi subduction zone, due to the significance of its contribution to the New Zealand tsunami hazard.

Obtaining more detail by further reduction in the length of the coastal sections used, currently 20 km, would be beneficial, as tsunami impacts may vary considerably even on this scale. It would be particularly helpful to be able to scale the hazard analysis to define separate coastal sections for the interior of the Waitemata and Wellington harbours. This would require refining of the associated numerical modelling grids in order to more accurately represent the harbour entrances.

6.12 REFERENCES

Abe, K. (1979). Size of great earthquakes of 1837–1974 inferred from tsunami data, *Journal of Geophysical Research*, 84, 1561-1568.

Abe, K (1981). Physical size of tsunamigenic earthquakes of the northwestern Pacific, *Physics of the Earth and Planetary Interiors* 27, 194-205.

Abe, K. (1985). Quantification of major earthquake tsunamis of the Japan Sea, *Physics of the Earth and Planetary Interiors*, 38, 214-223.

Abe, K. (1995). Estimate of tsunami run-up heights from earthquake magnitudes, In *Tsunami: Progress in Prediction, Disaster Prevention and Warning*, Y. Tsuchiya and N. Shuto (eds.), Kluwer Academic Publishers, 21-35.

Geist, E.L. (2002). Complex earthquake rupture and local tsunamis, *Journal of Geophysical Research*, 107(B5), 2086, doi:10.1029/2000JB000139.

Mueller, C.;, Power, W.; Fraser, S.; Wang, X. (2012). Towards a Robust Framework for Probabilistic Tsunami Hazard Assessment (PTHA) for Local and Regional Tsunami in New Zealand. Abstract volume of the Geosciences 2012 conference, Hamilton, New Zealand.p. 64.

Power, W.L.; Gale, N.H.; Lukovic, B.; Gledhill, K.R.; Clitheroe, G.; Berryman, K.R.; Prasetya, G. (2010) Use of numerical models to inform distant-source tsunami warnings. Lower Hutt: GNS Science. GNS Science report 2010/11. 22 p.

Satake, K.; Okada, M.; Abe, K. (1988). Tide gauge response to tsunamis: Measurements at 40 tide gauge stations in Japan, *Journal of Marine Research* 46, 557-571.

Stirling, M.; McVerry, G.; Gerstenberger, M.; Litchfield, N.; Van Dissen, R.; Berryman, K.; Barnes, P.; Beavan, J.; Bradley, B.; Clark, K.; Jacobs, K.; Lamarche, G.; Langridge, R.; Nicol, A.; Nodder, S.; Pettinga, J.; Reyners, M.; Rhoades, D.; Smith, W.; Villamor, P.; Wallace, L. (2012). National seismic hazard model for New Zealand: 2010 update, *Bulletin of the Seismological Society of America*, 102(4), 1514-1542.

Wang, X. ; Liu, P.L.-F. (2006). An analysis of 2004 Sumatra earthquake fault plane mechanisms and Indian Ocean tsunami. *Journal of Hydraulic Research*, 44(2), 147-154.

Wang, X.; Liu, P.L.-F.(2007). Numerical simulations of the 2004 Indian Ocean tsunamis - coastal effects. *Journal of Earthquake and Tsunami*, 1(3), 273-297.

This page is intentionally left blank.